จุฬาลงกรณ์มหาวิทยาลัย

ทุนวิจัย

กองทุนรัชดาภิเษกสมโภช

รายงานวิจัย

ผลของปริมาณเอท็อกซิเลตบิสฟีนอลเอไดเมธาคริเลตต่อสมบัติทางความร้อนและสมบัติเชิงกลพลวัตของพอลิแลคติคแอซิดโครงข่าย

โดย

รัตนวรรณ มกรพันธุ์

มิถุนายน 2558

Acknowledgements

The author would like to express my sincere gratitude to the Rachadapisek Sompoch Endowment, Chulalongkorn University, Thailand for funding support of this research. Furthermore, I would like to express my appreciation to The Petroleum and Petrochemical College, Chulalongkorn University, Thailand.

I would like to thank Associate Professor Dr Joao Maia who supported the rheological laboratory in department of Macromolecular Science and Engineering, Case Western Reserve University, Cleveland, Ohio, USA.

ชื่อโครงการวิจัย ผลของปริมาณเอท็อกซิเลตบิสฟีนอลเอไดเมธาคริเลตต่อสมบัติทางความร้อนและสมบัติเชิงกลพลวัตของพอลิแลคติคแอซิดโครงข่าย

ชื่อผู้ทำวิจัย รองศาสตราจารย์ ดร. รัตนวรรณ มกรพันธุ์

เดือนปีที่ทำวิจัย มิถุนายน 2558

บทคัดย่อ

การศึกษาพอลิแลกติคแอซิดแบบเชื่อมขวางทางเคมีด้วยสารที่ทำให้เกิดการเชื่อมขวาง โดยใช้ dicumyl peroxide (DCP) เป็นสารริเริ่มปฏิกิริยาและ ethoxylated bisphenol A dimethacrylates (Bis–EMAs) ทำหน้าที่เป็นสารเชื่อมขวาง ผลการศึกษาสมบัติการไหลพบว่าการเติม DCP ในพอลิแลกติคแอซิดปริมาณ 3 phr ทำให้มอดุลัสและความหนืดเชิงซ้อนเพิ่มขึ้นเมื่อเปรียบเทียบกับพอลิแลกติคแอซิด นอกจากนี้การเติม Bis–EMAs ในระบบ DCP/PLAพบว่าการเติม Bis–EMAs ในปริมาณ 5 phr จะส่งผลให้มอดุลัสและความหนืดเชิงซ้อนเพิ่มขึ้นเนื่องจากพอลิแลกติคแอซิดได้เกิดโครงสร้างแบบเชื่อมขวางขึ้น นอกจากนี้ผลการศึกษาสมบัติทางความร้อนพบว่าเสถียรภาพทางความร้อนของพอลิแลกติกแอซิคแบบเชื่อมขวางทางเคมีไม่เปลี่ยนแปลงเมื่อเปรียบเทียบกับพอลิแลกติกแอซิค ส่วนอุณหภูมิการเปลี่ยนสถานะคล้ายแก้วและอุณหภูมิตกผลึกเย็นของพอลิแลกติกแอซิคแบบเชื่อมขวางทางเคมีเพิ่มขึ้นเล็กน้อย และการศึกษาสมบัติเชิงกลพบว่าการเติม DCP และ Bis–EMAs ในพอลิแลกติกแอซิคส่งผลให้มอดุลัสเพิ่มขึ้นในขณะที่การยืดตัวที่จุดขาดลดลง นอกจากนี้สมบัติเชิงกลพลวัตพบการปรับปรุงประสิทธิภาพการทำงานของพอลิแลกติกแอซิคแบบเชื่อมขวางทางเคมีที่อุณหภูมิสูง ซึ่งในงานวิจัยนี้แสดงให้เห็นว่าพอลิแลกติกแอซิคแบบเชื่อมขวางทางเคมีมีสมบัติการไหล สมบัติทางความร้อน สมบัติเชิงกลและสมบัติเชิงกลพลวัตปรับปรุงขึ้นเมื่อเติมสารเชื่อมขวางปริมาณ 5 phr

Project Title	The Effects of Ethoxylated Bisphenol A Dimethacrylates Content on the Thermal and Thermo-mechanical Properties of Chemical Crosslinked Polylactic acid
Name of Investigator	Associate Professor Rathanawan Magaraphan
Year	June 2015

Abstract

Crosslinking structures of PLA can be effectively introduced into PLA by melt mixing using the initiation of dicumyl peroxide (DCP) in the presence of ethoxylated bisphenol A dimethacrylates (Bis–EMAs) which was used as a crosslinking agent. The results showed that the introduction of DCP into PLA above 3 phr increased storage modulus and complex viscosity when compared to PLA. DCP/PLA in the presence of Bis–EMAs content showed the optimum of storage modulus and complex viscosity were at a 5 phr Bis–EMAs loading and decreased as more Bis–EMAs were incorporated into DCP/PLA. The thermal stability of DCP/PLA/Bis–EMAs did not change when compared to PLA. Moreover, glass transition and cold crystallization temperatures of 0.3DCP/PLA/Bis–EMAs and 0.5DCP/PLA/Bis–EMAs slightly increased with increasing Bis–EMAs content. The crystallinity of DCP/PLA and DCP/PLA/Bis–EMAs were lower than that of PLA. The introductions of DCP and Bis–EMAs into PLA showed an increase of Young's modulus and a decrease of elongation at break. In addition, the dynamic mechanical properties revealed the improvement in high-temperature performance efficiency of the crosslinked PLAs where, in this work, their flow, thermal, mechanical and dynamic mechanical properties increased with increasing Bis–EMAs content up to 5 phr.

Keywords: Polylactic acid, Ethoxylated bisphenol A dimethacrylates, Chemical crosslinking, Rheological properties

Table of Contents

List of Tables

List of Figures

List of Figures

Page

List of Figures Page

List of Schemes

1. Introduction

Polylactic acid (PLA) is biodegradable polymer which are biocompatibility, biodegradability as well as superiority to mechanical properties over other conventional materials such as polyethylene [1]. In general, it is widely used in various applications, which are packaging, medical device, and textile, based on the environmental friendly materials. However, the poor thermal properties limited its applications. So, the thermal stability of PLA must be improved. Many techniques use to enhance this property of PLA, which are polymerization, graft copolymerization, and chain extender [2, 3]. These techniques provide a high molecular weight PLA. Hence PLA has high molecular weight; it can be enhanced thermal stability. Chemical crosslinking is another technique utilized to improve thermal stability of PLA. This technique provides the network structure of PLA [4]. The network structure can be retarded chain mobility and also increased thermal stability of PLA. This technique is economically advantageous because it was carried out in the melt state via extrusion process with only low amounts of crosslinking agent and no extra purification step and special apparatus were necessary.

The crosslinking structure of PLA was widely introduced by irradiation (γ−irradiation or electron beam irradiation) in the presence of various crosslinking agent e.g. triallyl isocyanurate (TAIC), trimethylallyl isocyanurate (TMAIC), trimethylolpropane triacrylate (TMPTA), and 1,6-Hexanediol diacrylate (HDDA) [5]. Many researchers found that TAIC are a good crosslinking agent for PLA to introduced crosslinking structure via irradiation method. According to Quynh et al. [6], they reported that the radiation dose of 30 kGy is the maximum dose to introduced crosslinking structure PLLA in the presence of 3 %wt TAIC. Mitomo et al. [5] also found that PLLA/3 %wt TAIC irradiated at 50 kGy showed improvement in heat stability above glass transition temperature.

In addition, the crosslinking structure of PLA can be formed by chemical crosslinking in the presence of a small amount of initiator and crosslinking agent via

extrusion process [7]. In general, crosslinked PLA can be introduced by peroxides that were decomposed and generated free radicals during the melt blending. Thus, these free radicals can react with PLA chains which have three possible ways of reactions, containing chain scission, branching, crosslinking reaction, or combination of three reactions to occur at the same time. As the reported by Zenkiewicz et al. [8], the addition of dicumyl peroxide (DCP) up to 0.4 %wt into PLA showed increase gel fraction of PLA up to 93 % which was a desirable crosslinking reaction. And gel fraction of PLA became decrease to 82 % with increasing DCP content over 0.4 %wt, thus caused undesirable crosslinking reaction.

Moreover, the rheological properties are important to understand the structure–property relationship in the crosslinking materials. According to Changgang et al. [9] found that the introduction of DCP into PLA showed higher storage modulus and complex viscosity than that of PLA at all frequency and gel–3D structure was formed. The complex viscosity and storage modulus of DCP/PLA blend increased with DCP content up to 0.5 %wt at low frequency because the incorporation of DCP can be introduced crosslinking structure between PLA chains that have been reported in Huang et al. [10]. In recently, crosslinked PLA with the introduction of DCP and crosslinking agents can form a gel structure as a reported by Yang et al. [4]. They found that gel fraction of crosslinked PLA started at 0.15 %wt of TAIC and 0.2 %wt 0f DCP and the increasing gel fraction resulted in developed storage modulus in glassy state and improved thermal stability.

This work was to introduce crosslinking structure of PLA in the presence of small amounts of bisphenol A ethoxylate dimethacrylate (Bis−EMAs) as a crosslinking agent and DCP via extrusion, aiming at improving the thermal and rheological properties. The effect of DCP and Bis−EMAs content on the rheological, thermal, mechanical, thermo–mechanical, and morphological properties was investigated.

2. Literature Review

2.1 Polylactic Acid

Polylactic acid or polylactide (PLA) is a thermoplastic aliphatic polyester derived from renewable resources, such as corn starch, tapioca products or sugarcanes. The fermentation of those renewable resources is produced lactic acid. The PLA chemical structure (Scheme 2.1) significantly depends on the way the technological process of polymerization of a monomer, i.e., lactide (LA), was performed. Scheme 2.2 shows the reaction to produce PLA. As a result, different forms of PLA may be obtained. These are as follows:

L(+)PLA, where each monomeric unit of a PLA macromolecule shows a specific rotation L.

D(–)PLA, where each monomeric unit of a PLA macromolecule shows a specific rotation D

L,D PLA, where monomeric units of a PLA macromolecule show both specific rotations (either L or D).

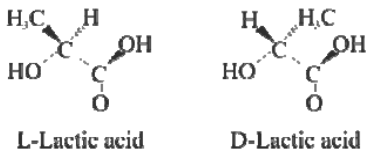

Scheme 2.1 PLA chemical structure.

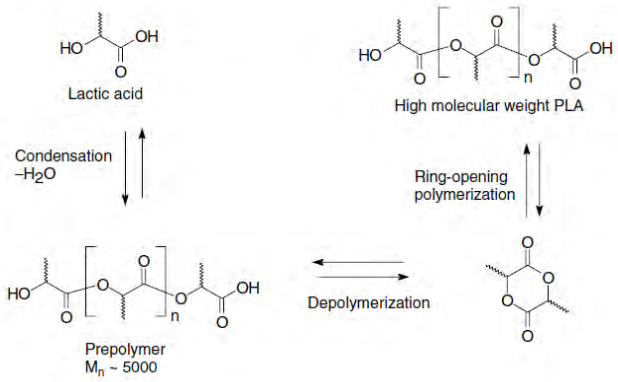

Scheme 2.2 Reaction schemes to produce PLA.

2.1.1 PLA Physical Properties

The physical characteristics of high molecular weight PLA are to a great extent dependent on its transition temperatures for common qualities such as density, heat capacity, mechanical, and rheological properties. In the solid state, PLA can be either amorphous or semicrystalline, depending on the stereochemistry and thermal history. For amorphous PLA, the glass transition (T_g) determines the upper use temperature for most commercial applications. For semicrystalline PLA, both the T_g (~58 ºC) and melting point (T_m), 130 ºC–230 ºC (depending on structure) are important for determining the use temperatures across various applications. Both of these transitions, T_g and T_m, are strongly affected by overall optical composition, primary structure, thermal history, and molecular weight. Above T_g amorphous PLA transition from glassy to rubbery and will behave as a viscous fluid upon further heating. Below T_g, PLA behaves as a glass with the ability to creep until cooled to its β transition temperature of approximately −45 ºC. Below this temperature PLA will only behave as a brittle polymer.

2.1.2 Degradation and Hydrolysis

Under conditions of high temperature and high humidity, as in active compost, for example, PLA will degrade quickly and disintegrate within weeks to months. The primary mechanism of degradation is hydrolysis, followed by bacterial attack on the fragmented residues.

In the first stage, degradation of PLA is primarily due to hydrolysis of the ester linkages, which occurs more or less randomly along the backbone of the polymer. It requires the presence of water according to the following reaction:

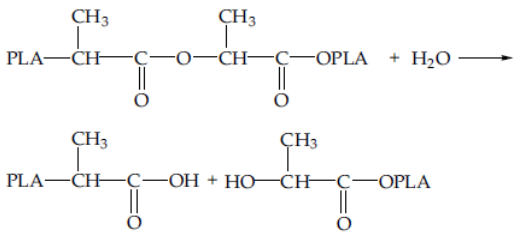

Scheme 2.3 Hydrolysis of the ester linkages of PLA.

In the second stage, the enzymatic degradation proceeded via mainly a surface erosion mechanism. Amorphous regions hydrolyzed more readily than crystalline regions.

Aerobic biodegradation (such as composting)

$$\text{Polymer} + O_2 \rightarrow CO_2 + H_2O$$

Anaerobic biodegradation (such as landfill and anaerobic digestion)

$$\text{Polymer} \rightarrow CO_2 + CH_4 + H_2O$$

The environmental degradation of PLA occurs by a two−step process. During the initial phases of degradation, the high molecular weight polyester chains hydrolyze to lower molecular weight oligomers. The rate of hydrolysis is accelerated by acids or bases and is dependent on moisture content and temperature. Article

dimensions, crystallinity, and blends will affect the rate of degradation. PLA products rapidly degrade in both aerobic and anaerobic composting conditions.

2.1.3 Applications and Performance

Since PLA is an environmentally friendly polymer that can be designed to controllably biodegrade, it is ideally suited for many applications in the environment where recovery of the product is not practical, such as agricultural mulch films and bags. Composting of post−consumer PLA items is also a viable solution for many PLA products. However, the large growth seen for PLA in many applications does not depend upon the biodegradability of the material.

PLA resins can be tailor−made for different fabrication processes, including injection molding, sheet extrusion, blow molding, thermoforming, film forming, or fiber spinning. The key is controlling certain molecular parameters in the process such as branching, D−isomer content, and molecular weight distribution. The ability to selectively incorporate L−, D−, or meso−lactide stereoisomers into the polymer backbone allows PLA to be tailored for specific applications. The ease of incorporation of various defects into PLA allows for control of both crystallization rate and ultimate crystallinity.

Films are the second largest application area for PLA. Again, the ability to modify the crystallization kinetics and physical properties for a broad range of applications by D− or meso−comonomer incorporation, branching, and molecular weight change makes PLA extremely versatile. Films are transparent when stress crystallized and have acceptance by customers for food contact. PLA films can be prepared by blown double bubble technology or preferably, cast−tentering. Cast−tentered films have very low haze, excellent gloss, and gas (O_2, CO_2, and H_2O) transmission rates desirable for consumer food packaging. PLA films also have superior dead fold or twist retention for twist wrap packaging [11].

Tsuji *et al.* (1999) [12] studied films of 1:1 blend and films non−blended were prepared from poly(L–lactic acid) (PLLA) and poly(D−lactic acid) (PDLA) with a

solution casting method. The result showed the T_g of blend films is 58 ºC higher than that for non−blended films with M_w in the range $5x10^4$–$1x10^5$, where predominant stereocomplexation occurs in the blend films. Moreover, T_m of stereocomplex crystallites of blend films has a maximum at M_w of around $1x10^5$, while T_m of homo−crystallites monotonously increases with the increasing M_w. This suggests that the crystalline thickness of the stereocomplex crystallites in blend films becomes the highest at M_w of around $1x10^5$. The enthalpy of melting for stereocomplex crystallites in 1:1 blend films was higher than that of homo−crystallites when M_w of polymers was below $2x10^5$, while this relationship was reversed when M_w increased to $1x10^6$.

Anderson *et al.* (2006) [13] studied melt blending procedure was developed for the preparation of PLLA/PDLA stereocomplex crystallites dispersed in a PLLA matrix. The result showed the T_m of the PLLA homopolymer is present around 173.8 ºC, while the stereocomplex T_m, around 215.8 ºC. The area of the melting endotherm for the stereocomplex decreased as the amount of PDLA in the blend decreased showing that the initial composition of the blend can be used to control the amount of stereocomplex in the final material. The blends with the intermediate molecular weight, 3 wt% of the 14 kg mol/K PDLA, stood out as having the highest nucleation efficiencies and smallest half–time values, indicating that there may be an optimum molecular weight of the PDLA for stereocomplex nucleating agents. All of the blends containing the stereocomplex showed more significant improvements in the crystallization rate of PLLA compared to talc.

Yokohara *et al.* (2008) [14] studied structure and properties for binary blends composed of PLA and poly(butylene succinate) (PBS) by an internal batch mixer. It found that PLA and PBS are immiscible in the molten state and the blends exhibit phase−separated structure. The addition of PBS enhances the crystallization of PLA because PBS droplets act as crystallization nuclei. In addition, the enhancement of the storage modulus due to the cold crystallization of PLA is shifted to lower temperature by blending PBS. This phenomenon indicates that PBS accelerates cold crystallization of PLA.

Ren *et al.* (2009) [15] studied biodegradable binary and ternary blends of thermoplastic starch (TPS), PLA, and poly(butylene adipateco-terephthalate) (PBAT) give excellent properties when small amount of compatibilizer (anhydride functionalized polyester) is added. It showed that as PBAT content increased, the value of the storage modulus (E') of the blends decreased, which indicated that the blends with less PBAT content were more elastic than those with more PBAT content. The T_g showed a slight decrease with increasing PBAT content. In addition, the vicat softening temperature (VST) increased with the PBAT content. It is because PBAT has higher VST than PLA.

Chang *et al.* (2011) [16] studied the effects of poly(3-hydroxybutyrate) (PHB) on crystalline morphology of stereocomplex capacity of PLLA and PDLA were prepared using solvent−mixing, followed with film−casting. The neat stereocomplexed PLA (sc−PLA) exhibited T_g around 40 ºC, and T_m at about 221 ºC. The PHB/sc−PLA blend showed crystallization growth of sc−PLA in blends is hindered by presence of PHB and final morphology of the sc–PLA complexes is altered. The less perfect lamellae of sc−PLA formed in blends induced by the increase of PHB content in blends or higher T_c. In addition, the sc−PLA in blends melt−crystallized at 170 ºC, show coexistence of feather−like and wedge−like spherulites. The concentration and/or distribution of the PHB (amorphous diluents) at the crystal growth front corresponding to variation of the slopes of spherulitic growth rates is a factor which results in the different orientation of sc−PLA lamellae in blends.

2.2 Crosslinking

Crosslinking is the formation of chemical links between molecular chains to form a three−dimensional network of connected molecules. The establishment of chemical bonds between polymer molecule chains may be accomplished by heat, vulcanization, irradiation or the addition of a suitable chemical agent. Crosslinking restricts chains from sliding past one another and generates elasticity in an amorphous polymer. It makes a polymer more resistant to heat, light, and other physical agencies, giving it a high degree of dimensional stability, mechanical strength and chemical and

solvent resistance. The effects of crosslinking on the physical properties of the polymers are primarily influenced by the degree of crosslinking, the regularity of the network formed, and the presence and absence of crystallinity in the polymer. For crystalline polymers there may be a reduction in crystallinity with a low degree of crosslinking as it hinders chain orientation, and the polymer may become softer, more elastic, and have a lower melting point. Crosslinking changes the local molecular packing and leads to a decrease in free volume. This is reflected in an enhancement of glass transition temperature. Improvement in creep behavior also results from crosslinking as it restricts the viscous flow [17]

Advantages of crosslinking:

1. Higher tensile strength
2. Improved abrasion/cut through
3. Better crush resistance
4. Solder iron resistance
5. Better over load characteristics
6. Resistance to stress cracking
7. Improved fluid resistance
8. Slightly better flame resistance
9. No change of electrical
10. Negligible change in thermal stability
11. Decrease in flexibility
12. Improved high temperature mechanicals

2.2.1 Chemical Crosslinking

Chemical crosslinking is another possible way to introduce crosslinking structures. Some chemical reactions between the crosslinking agent and the polymer chains can be initiated by chemical treatments without irradiation, and modified materials with different gel fraction and crosslinking density for further processing of products can be obtained [4]

The chemical methods, peroxide induced crosslinking, which has been widely applied through the addition of small amount of peroxide during extrusion. By reactive extrusion peroxides decompose forming free radicals. These radicals present in polymer matrix can promote chain scission, branching, crosslinking or any combination of the three. These reactions will influence physical properties such as melt viscosity, crystallinity, glass transition temperature, melting temperature, tensile and impact

strengths [18]. For example, the crosslinking structures could be effectively introduced to PLA by initiation of dicumyl peroxide (DCP) in the presence of small amount of crosslinking agent (triallyl isocyanurate), and crosslinked PLA with significantly improved thermal stability and enhanced tensile strength [7].

2.2.2 Crosslinking Agent

The thermal stability of PLA can be significantly improved by the chemical crosslinking of PLA containing suitable concentration of various crosslinking agents such as TAIC, TMAIC, and TMPTA. Scheme 2.4 lists structural formulae of prominent crosslinking agents for PLA. These agents all have multifunctional groups, which can react with polymer chains to form crosslinks [19].

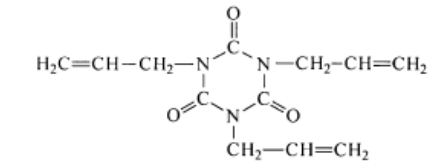

Triallyl isocyanurate (TAIC)

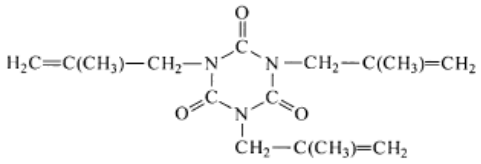

Trimethylallyl isocyanurate (TMAIC)

$H_2C{=}CHCO_2CH_2)_3CC_2H_5$

Trimethylolpropane triacrylate (TMPTA)

$[H_2C{=}C(CH_3)CO_2CH_2]_3CC_2H_5$

Trimethylolpropane trimethacrylate (TMPTMA)

$[H_2C{=}CHCO_2(CH_2)_3-]_2$

1,6-Hexanediol diacrylate (HDDA)

$[CH_2[OCH_2CH(CH_2OCH_2CH{=}CH_2)]_5OH]_2$

Ethylene glycol bis [pentakis (glycidyl allyl ether)] ether, hydroxy terminated (EG)

Scheme 2.4 Structural formulae of multifunctional crosslinking agents.

2.2.3 Ethoxylated Bisphenol A Dimethacrylates (Bis–EMAs) Molecular Weight = 376

The use of resin adhesives containing low shrinkage crosslinking monomers such as ethoxylated bisphenol A dimethacrylates also facilitates the placement of resin composite restorations preventing excessive stress of contraction subsequent.

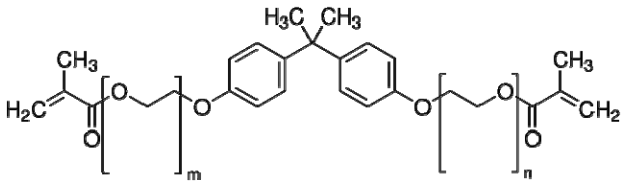

Scheme 2.5 Structural of Bis−EMAs.

Bis−EMAs can be used as a crosslinking agent and chain extender at the same time and a highly effective crosslinker. It can be carried out with conventional peroxides or irradiation. The resulting polymers have improved mechanical properties, as well as improved chemical and high temperature resistance [20]

2.2.4 Measurement of Gel Fraction

Gel fraction was measured by the weight remaining after dissolving the sample in chloroform using the following eq. 2.1

$$Gelfraction = \left(\frac{W_g}{W_0} \right) \times 100 \qquad (2.1)$$

where W_0 is initial weight (dry), W_g is the remaining weight (dry gel component) of the crosslinked sample after dissolving in chloroform at room temperature for 24 h.

2.2.5 Time Temperature Transformation (TTT) Diagram

For processing purposes, the gel points represents the state beyond which the material no longer flows and is therefore incapable of being processed. Gelation does not involve any change in the curing process (the reaction rate is unmodified), and therefore cannot be detected by techniques sensitive to chemical reaction, such as differential scanning calorimetry (DSC). However, the mechanical and viscoelastic properties of the reaction medium do change during gelation, which can therefore be detected by methods based on changes in these properties. It is generally accepted that gelation occurs at a fixed conversion value which is independent of the curing temperature and depends on the functionality, reactivity, and stoichiometry of the reactive species. Vitrification is understood as a change from the liquid or rubbery state to the glassy state due to an increase in both crosslinking density and the molecular weight of the material during the curing process.

This transformation occurs when the T_g of the material coincides with the curing temperature. As of this moment, curing within the glassy state becomes extremely slow and the reactive process changes from chemical control to control by diffusion. The different states the material can pass through during the curing process can be represented in the time-temperature-transformation (TTT) diagram. For the construction of the TTT diagram it is necessary to know the curing kinetics up to when the material vitrifies and also the gel time (t_{gel}) and vitrification time (t_{vit}). Three characteristic temperatures exist in the TTT diagram: T_{go}, the glassy transition temperature of the material without crosslinking; ${}_{gel}T_g$, the lowest curing temperature which allows material to gel before it vitrifies, which coincides with the curing temperature at which the material gels and vitrifies simultaneously; and $T_{g\infty}$, the highest glassy transition temperature, or lowest temperature at which complete curing can be achieved. Below T_{go} the material does not crosslink. Between T_{go} and ${}_{gel}T_g$ the liquid resin reacts until the glassy transition temperature coincides with the curing temperature; at this moment vitrification begins and the reaction changes to control by diffusion. Between ${}_{gel}T_g$ and $T_{g\infty}$, the material first gels and then vitrifies when $T_c = T_g$. Above $T_{g\infty}$

the material is completely cured and remains in the rubbery state after gelling. Figure 2.1 shows the example of TTT diagram of unsaturated polyester resin. The TTT diagram can be described with the Arrhenius equation:

$$ln\ t = A + E/RT. \qquad (2.2)$$

where t is time, A is Arrhenius constant, E is the activation energy, R is the universal gas constant, and T is temperature [21, 22].

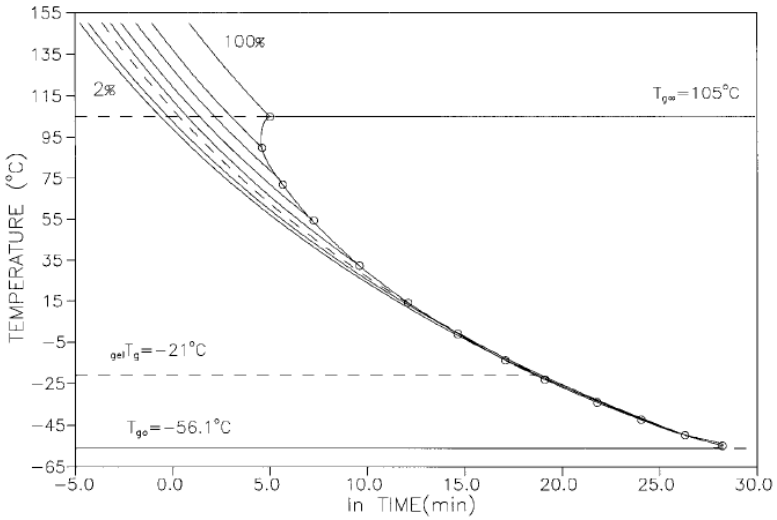

Figure 2.1 TTT cure diagram for unsaturated polyester resin cured with 1.5% of benzoyl peroxide as an initiator.

2.2.6 Crosslinking Polymer at The Gel Point

2.2.6.1 Linear Viscoelaticity and Oscillatory Shear Experiments.

When oscillatory shear measurements are performed in the linear viscoelastic regime, the storage modulus G' (elastic response) and loss modulus G" (viscous behavior) are independent of the strain amplitude.

An oscillatory shear experiment, which is exposed to a sinusoidal strain (γ) at an angular frequency of ω will respond with a gradual approach to a steady sinusoidal stress (σ)

$$\gamma = \gamma_0 \sin \omega t \tag{2.3}$$

$$\sigma = \gamma_0 (G'(\omega) \sin \omega t + G''(\omega) \cos(\omega t)) \tag{2.4}$$

From this type of experiment the storage modulus G', the loss modulus G" and the dynamic viscosity $\eta' = G''/\omega$ can be determined. These are generally repersentes in terms of the elastic G', viscous G", and complex shear modulus G*:

$$G' \alpha \sin \omega t \,,\; G'' \alpha \cos \omega t \,,\; G^* = (G'^2 + G''^2)^{1/2} \tag{2.5}$$

$$\text{Loss tangent: } \tan \delta = \frac{G''}{G'} \text{ (measure of damping)} \tag{2.6}$$

2.2.6.2 Theoretical Models for Linear Viscoelasticity

In the linear viscoelastic regime (small strain values) the viscoelastic properties of the incipient gel can be described by the gel equation $(-\infty < t' < t)$.

$$m(t) = S \int_{-\infty}^{t} (t - t')^n \gamma(t') dt' \tag{2.7}$$

when m = the shear stress

$\gamma(t')$ = the rate of deformation of the sample

S = the gel strength parameter (depends on the crosslinking density and the molecular chain flexibility)

n = the relaxation exponent

For incipient gels G' and G" are expected to obey power laws in frequency: $G' \sim G'' \sim \omega^n$

The gel point of a chemical gel can be determined by observation of a frequency independent value of tan δ versus time or versus temperature for a thermo–reversible gel.

An alternative method is to plot against temperature the apparent viscoelastic exponents n' and n" obtained from the frequency dependence of G' and G" at each temperature of measurement and observing a crossover where n'=n"=n.

2.2.6.3 The Behavior at The Gel Point of Crosslinking Polymer

Crosslinking polymers undergo phase transition from liquid to solid at critical extent of reaction. This phenomenon is called gelation. The polymer is said to be at the gel point (GP) if its steady shear viscosity is infinite and its equilibrium modulus is zero. Several processes may contribute to this transition besides the connecting of molecular strands by chemical crosslinking: physical entanglements between the macromolecular strands, vitrification as the glass transition temperature rises with increasing extent of reaction, phase separation of the reaction components or products, and crystallization [23].

To determine the gel point during a crosslinking reaction, the complex moduli are measured as a function of time as shown in Fingure 2.12. At early times, both of moduli are low and the elastic portion G' is much smaller than the viscous portion G". This is characteristic of a polymer liquid at low frequencies. The presence of a small elastic contribution well before the critical gel point is due to the stretching of the polymers under deformation and potentially physical entanglements between the polymers. As the crosslinking reaction progresses, the molecular weight of the polymers increases, increasing both the viscosity and relative contribution of the elastic modulus G'. Longer polymers have longer relaxations times and more entanglements. At a time

known as the cross–over point, the elastic modulus becomes larger than the viscous modulus. As the reaction progresses to completion, the elastic and viscous moduli approach their equilibrium values. Stiffer gels will have a higher elastic modulus and a smaller phase angle δ. In the limit of a very stiff gel, the viscous contribution may be negligible [9].

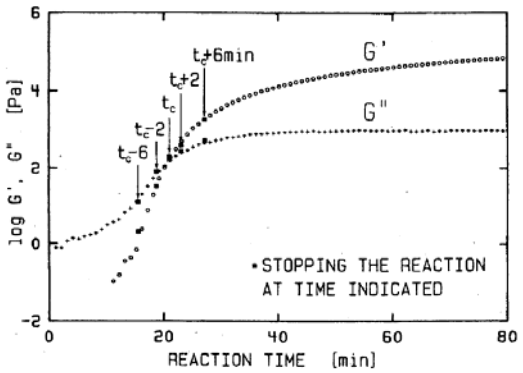

Figure 2.2 Shear moduli as a function of time during crosslinking reaction.

Yang *et al.* (2008) [2] studied thermal and mechanical properties of chemical crosslinked PLA. Crosslinking was introduced via chemical treatment of the melt by adding small amounts of crosslinking agent triallyl isocyanurate (TAIC) and dicumyl peroxide (DCP) as seen in Scheme 2.6. The results showed that the crosslinking of PLA started at a low content of either TAIC or DCP, resulting in a decrease of crystallinity and a significant improvement of the thermal degradation initiation and completion temperatures, which indicated better thermal stability than neat PLA. Crosslinking was also responsible for the improved tensile modulus and tensile strength.

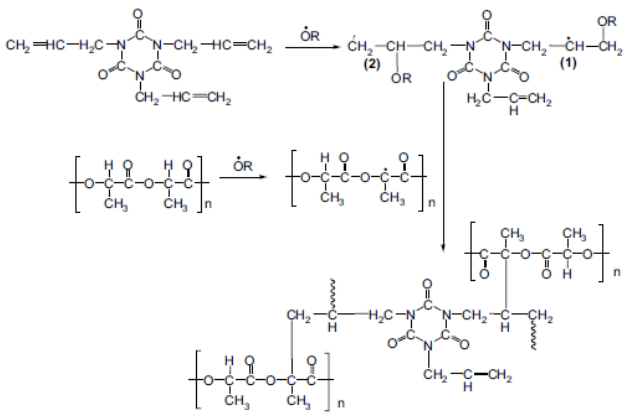

Scheme 2.6 One possibility of reaction scheme for chemical crosslinking of TAIC between two PLA molecules.

Quynh *et al.* (2007) [24] studied crosslinked PLA have been produced by radiation modification in the presence of a suitable crosslinker (TAIC). The results showed that the properties of crosslinked samples are governed by crosslinking density and these improvements seemed to increase with radiation dose. The melting and crystallinity peaks of crosslinked PLA decreased with the radiation dose and seemed to be non−crystalline. These decreases may be caused by reduction of degree of crystallization of polymer chains suggested that the molecular chains were crosslinked in the amorphous state. The crosslinking structure formed in irradiated samples of PLA containing TAIC resulted in a significant improvement of their mechanical properties.

Changgang et al. (2009) [9] studied the effects of dicumyl peroxide (DCP) at low concentrations on initiating crosslinking of polylactide (PLA) by melt blending. The results showed that the crosslink rate of the blends increased with DCP content increasing. The PLA gel with 0.73 wt% of DCP appeared obvious crystallization behavior and a new crystalline structure may be formed as DCP was 1.4 wt%. And it was also found that the exothermal peak temperature of PLA gel decreased with increasing DCP content except for the gel with 1.4 wt% of DCP. It also has been inferred by rheology analysis that the blend may be the structure of gel or 3D network.

Comparing to PLA melt, the G' and G" for the PLA with 1.1 wt% DCP were higher than PLA and increased with the frequencies increasing. The G' was enhanced and higher than G" at whole frequencies, meanwhile, the G' showed a “plateau” at low frequency. The results indicated that the PLA with 1.1 wt% DCP had a strong gel–3D network structure.

Young Shin *et al.* (2010) [25] studied the rheological and thermal properties of the PLA modified by electron beam irradiation in the presence of glycidyl methacrylate (GMA). In the case of irradiated virgin PLA, η* and G' seriously decreased with increasing irradiation dose and were much lower than those of virgin PLA due to the chain scission. However, the chain scission was suppressed and branching was enhanced by introducing the GMA. It was confirmed that a branching or a chain scission reaction was more dominant than a crosslinking reaction from the very low gel fraction in all tested samples. Compared to virgin PLA, irradiated PLA with 3 phr GMA had a η* of about 10 times higher and G' of 100 times higher than those of virgin PLA at 0.1 rad/s because of long chain branched structure. Gel fraction measurement revealed that chain scission and branching was more dominant than crosslinking.

3 Experimental

3.1 Materials

Polylactic acid, grade 4043D (ρ=1.25 g/cm^3 and T_m=210 ºC), was purchased from Nature−Work LLC. Dicumyl peroxide (DCP) with 99% purity was used as a radical initiaors and Bisphenol A ethoxylate dimethacrylate (Bis−EMAs) Mw 376 was used as a crosslinking agent, were purchased from Sigma−Aldrich.

3.2 Sample Preparation

PLA samples containing different concentrations of Bis−EMAs (1, 3, 5, and 7 phr) and DCP (0.1, 0.2, 0.3, 0.4, and 0.5 phr) were mixed in a corotating twin−screw extruder with an L/D ratio of 40 (LABTECH type LHFS1−271822) as shown in Figure 3.1. The temperature profile was maintained in the range of 140−190 ˚C from the feed throat to the die and the rotational speed was fixed at 10 rpm. Table 3.1 shows composition of each sample.

The rheological, thermo−mechanical, thermal (decomposition temperature), and morphological testing specimens were prepared by compression molding (Wabash, model V50H−18−CX) for 5 min at 200 ˚C and subsequently cooled under pressure by water circulation through the plates.

Figure 3.1 Preparation of crosslinked PLA via twin−screw extruder.

Table 3.1 Composition of each sample

DCP (phr)	Bis-EMAs (phr)	PLA (wt%)	Code
0	0	100	PLA
0.1	0	100	0.1DCP
0.2	0	100	0.2DCP
0.3	0	100	0.3DCP
0.4	0	100	0.4DCP
0.5	0	100	0.5DCP
0.1	1	100	0.1D1B
0.1	3	100	0.1D3B
0.1	5	100	0.1D5B
0.1	7	100	0.1D7B
0.3	1	100	0.3D1B
0.3	3	100	0.3D3B
0.3	5	100	0.3D5B
0.3	7	100	0.3D7B
0.5	1	100	0.5D1B
0.5	3	100	0.5D3B
0.5	5	100	0.5D5B
0.5	7	100	0.5D7B

3.3 Characterization

3.3.1 Measurement of Gel Fraction

- Dissolving sample pellet in chloroform at room temperature

Gel fraction was measured by the weight remaining after dissolving sample pellet in chloroform using the following eq. 3.1

$$Gelfraction = \left(\frac{W_g}{W_0} \right) \times 100 \qquad (3.1)$$

where W_0 is initial weight (dry), W_g is the remaining weight (dry gel component) of the crosslinked sample after dissolving in chloroform at room temperature for 24 h.

- Sohxlet extraction

The gel contents of the crosslinked samples (pellet) were determined by extracting the soluble fraction with boiling chloroform (61 ºC–62 ºC) for 2 h in a soxhlet extractor (SER 148). The gel fraction was calculated using eq. 3.1.

3.3.2 Rheological Measurement

The rheological properties were measured using Anton Paar Rheometer. The measurement was run using parallel plate (d= 25 mm) and the gap was set at 1mm. The samples were loaded between parallel plates and melted at 190 ºC for 2 min before compressed. Frequency sweeps between 0.1–100 rad/s were carried out at 5% strain which is the linear viscoelastic region of the measured samples. Time sweeps were carried out at 5% strain and at testing temperature of 150 ºC for 2 h, frequency of 1 Hz.

3.3.3 Thermogravimetric Analyzer (TGA)

Thermogravimetric analysis was carried out with a TA Instruments (Q500 TGA) under a nitrogen flow (40 ml/min). The samples were measured from 30 ºC to 600 ºC with a heating rate of 10 ºC/min. The decomposition temperature and temperature at

maximum rate of mass loss (T_{max}), of derivative thermogravimetric curve (DTG) were evaluated.

3.3.4 Differential Scanning Calorimeter (DSC)

Differential scanning calorimeter was performed using a Perkin−Elmer DSC 822 under N_2 atmosphere. The sample pellets were heated from 10 ºC to 200 ºC at a heating rate of 10 ºC/min. The glass transition temperature (T_g), cold crystallization temperature (T_{cc}), and melting temperature (T_m) of each specimens was recorded from the second run. The degree of crystallization (χ_c) was calculated as:

$$\chi_c = \frac{\Delta H_m - \Delta H_{cc}}{\Delta H_{m0} \times w} \times 100 \qquad (3.2)$$

where ΔH_m is the enthalpy of melting, ΔH_{cc} is the enthalpy of cold crystallization, ΔH_{m0} is enthalpy of melting for the 100% crystalline PLA, taken as 93 J/g, w is the weight fraction of PLA in samples [26].

3.3.5 Mechanical Testing

Tensile tests were performed using an Instron Universal Testing Machine (4206) with a crosshead speed of 50 mm/min. The specimens were prepared according to ASTM D638 standard.

Impact testing was performed according to ASTM D256 (notched type), and the impact strength was measured using the ZWICK 5113 pendulum impact tester with a pendulum load of 21.6 J.

3.3.6 Dynamic Mechanical Analyzer

Dynamic mechanical analysis (DMA) was performed using an EPLEXOR 100N in tension mode. The sample dimensions with a length of 40 mm, width of 10 mm, and thickness of 3 mm were used. The measurements were carried out at a constant

frequency of 1 Hz, strain amplitude of 0.1%, and a temperature range of 10 ºC to 120 ºC, with a heating rate of 2 ºC/min.

3.3.7 Morphological Observation

The material microstructure was examined using a field emission scanning electron microscope (FE–SEM; HITACHI S4800) with an acceleration voltage of 5 kV. The freeze–fractured ends of specimens were sputtering coated (HITHACHI E−1010) with a thin layer of platinum prior to analysis.

4. Results and Discussion

4.1 Chemical Crosslinking Reaction of PLA

For DCP/PLA system, the introduction of DCP is decomposed into free radicals during extrusion and PLA is created radicals by the abstraction hydrogen with radicals from peroxide. Thus the radicals from PLA can be generated and reacted with themselves to forming the crosslinking structure as seen in Scheme 4.1. However, radicals can be created at the tertiary hydrogen atom positions on PLA chains which is the possible way to promote chain scission [27].

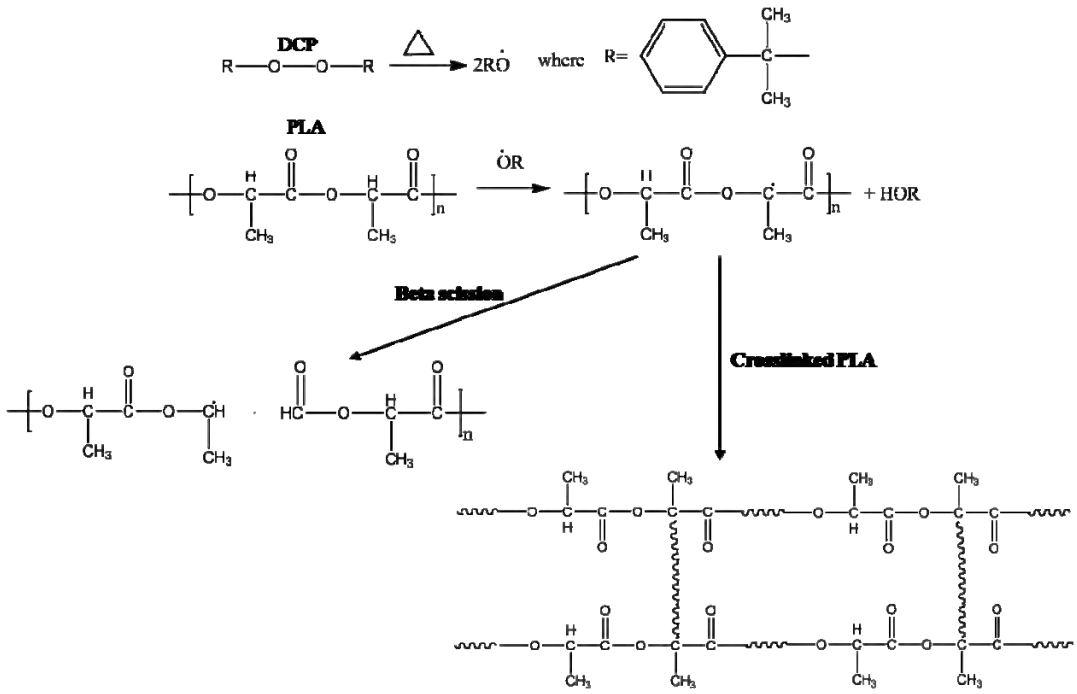

Scheme 4.1 Formations of chain scission and crosslinking structure of PLA in the presence of DCP.

The reaction of chemical crosslinking of PLA in the presence of Bis–EMAs (DCP/PLA/Bis–EMAs) was shown in Scheme 4.2. The double bonds in Bis–EMAs are broken and created two possible ways of radicals, which are usual way at position 1 and rare way at position 2. Then the radicals from Bis–EMAs reacted with radicals from PLA to create the chemical crosslinking reaction as seen in Scheme 4.2. The two competitive reactions can be occurred which consisted of branched PLA and crosslinked PLA structures. The branched PLA obtained from the loading low amount of Bis–EMAs while the crosslinked PLA obtained from the adding high amount of Bis–EMAs. At the same time, the combinations of branching and crosslinking reactions can be occurred [25].

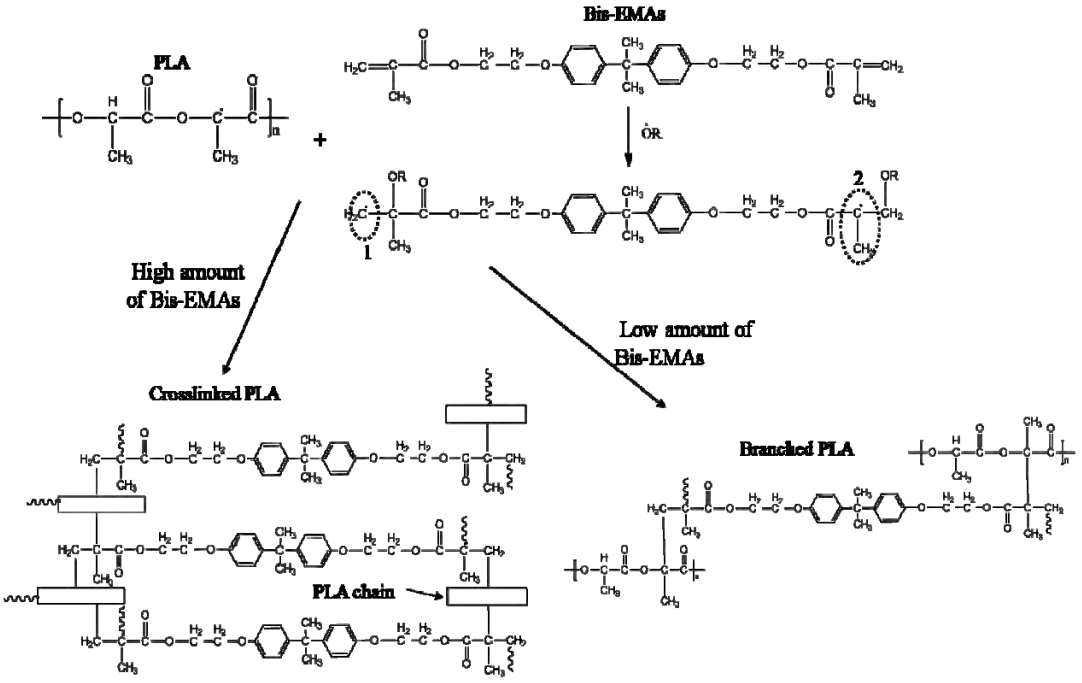

Scheme 4.2 The possibility of chemical crosslinking between Bis–EMAs and PLA.

4.2 Gel Fraction

Figure 4.1 shows the gel fraction of DCP/PLA. The result shows that DCP/PLA samples at room temperature condition are higher gel fractions than that of sohxlet extraction. This is due to the solubility of sample increased with the increasing temperature. Gel fractions at room temperature condition and sohxlet extraction show the same tendency. Moreover, gel fractions of DCP/PLA samples increased with the increasing DCP content. The values of gel fractions at room temperature condition are less than 60 % which are corresponding to low amount of crosslinking structure.

Gel fractions of DCP/PLA/Bis–EMAs at room temperature condition and sohxlet extraction are shown in Figure 4.2(a) and Figure 4.2(b), respectively. It can be seen that DCP/PLA/Bis–EMAs are higher gel fractions than that of DCP/PLA because the presence of Bis–EMAs as a crosslinking agent effectively enhanced the crosslinking structure. DCP/PLA/Bis–EMAs at room temperature condition (< 90 %) show higher gel fractions than sohxlet extraction (< 40 %). A high value of gel fraction suggests that there is a higher possibility to occur crosslinking structure than that of chain scission and branching structure. In addition, gel fractions of DCP/PLA/Bis–EMAs of both conditions increased with increasing Bis–EMAs up to 5 phr. Further increasing Bis–EMAs to 7 phr resulted in decrease gel fraction. It can be explained that the loading of Bis–EMAs over 5 phr is generated a large amount of radicals led to degradation of PLA chains. This situation is undesirable reaction for chemical crosslinking PLA in the presence of Bis–EMAs.

Figure 4.3 shows the pellets of PLA, DCP/PLA and DCP/PLA/Bis–EMAs samples. It can be known that gel is found in the crosslinking sample. PLA pellets did not observe gel. It can be seen that a high amounts of DCP and Bis–EMAs loading showed high amount of gel content in the sample. This result agrees with the gel fraction. Since gel in the samples increased that associated with increasing crosslinking structure, the sample pellets showed more opaque.

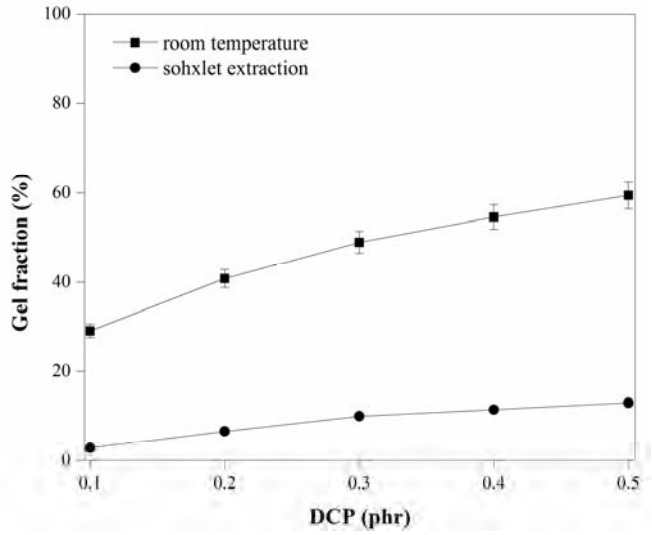

Figure 4.1 Gel fraction of DCP/PLA as a function of DCP content.

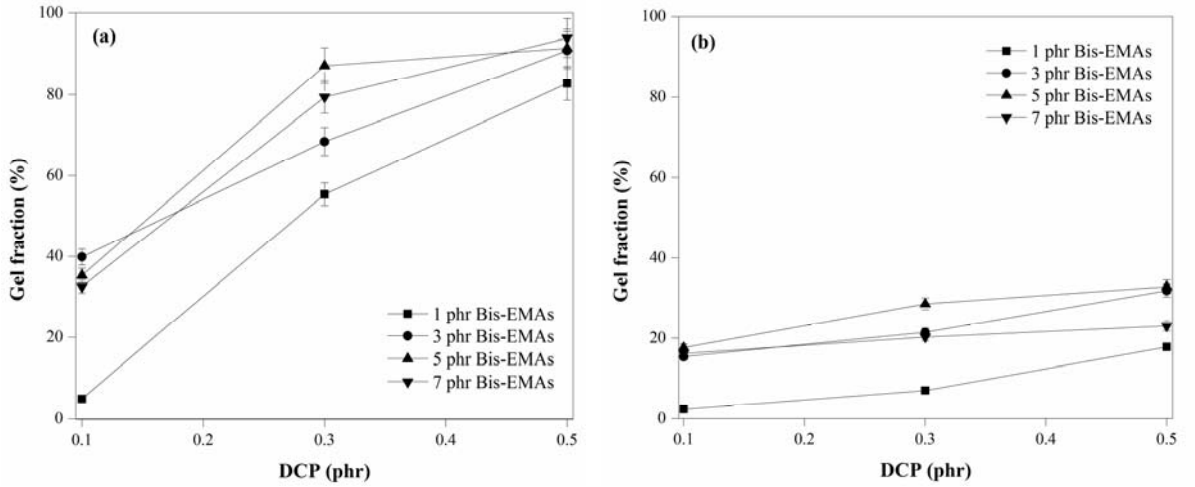

Figure 4.2 Gel fraction of chemical crosslinked PLA as a function of DCP content of (a) at room temperature and (b) after sohxlet extraction.

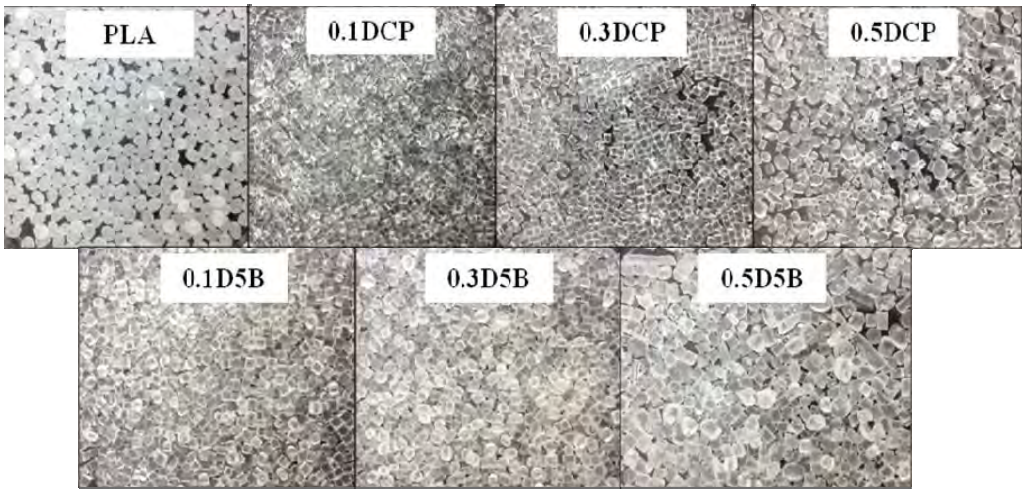

Figure 4.3 Images of PLA, DCP/PLA, and DCP/PLA/Bis–EMAs pellets**.**

4.3 Rheological Properties

4.3.1 Time Sweep

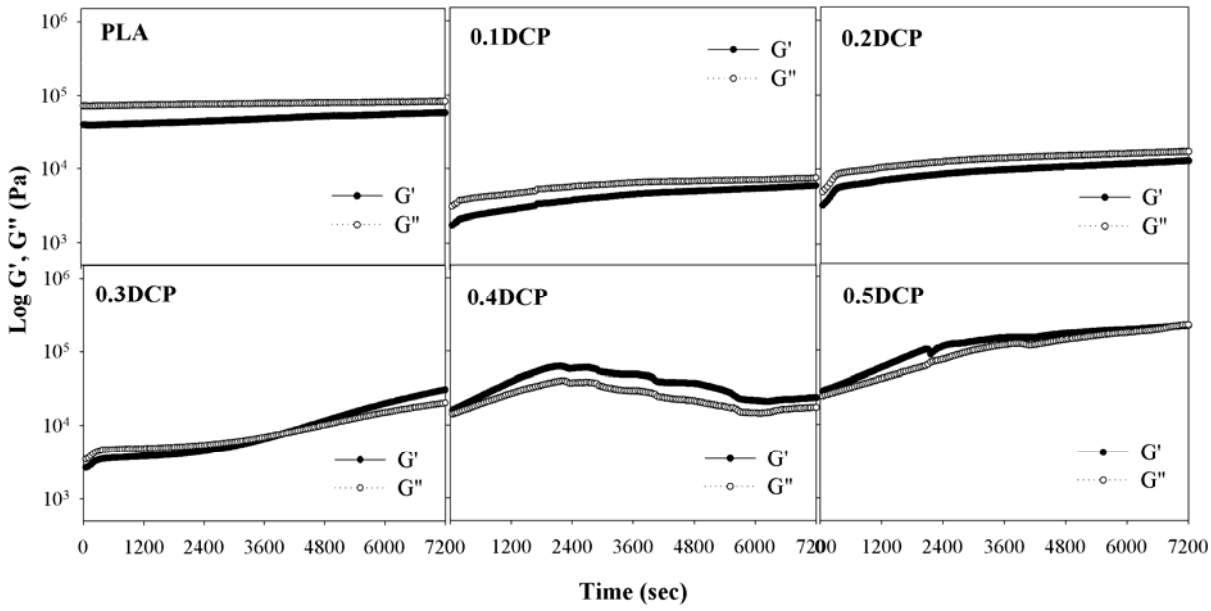

Figure 4.4 G' and G" as a function of time of PLA and DCP/PLA at 150 ºC.

Figure 4.4 shows the variation of the storage (G') and loss (G") modulus versus time at 150 °C. The crossover between G' and G" defines the gel point of a polymer chains form a three–dimensional network [23]. The results show that the G' and G" of PLA are parallel and G">G' is characteristics of polymer liquid. The addition of DCP at 3 phr observes the gel point (gel time~3940 s), indicates that the crosslinking reaction started at this point. At gel point, the G'=G" is about 7,670 Pa. Above the gel point, the G' increased and reached a steady state value corresponding to the end of the crosslinking reaction. In the case of 0.1DCP and 0.2DCP samples, they did not observe the gel point. It can be suggested that the addition of DCP below 0.3 phr is not sufficient to promote radical reaction. At above 0.3 phr DCP, the G' and G" are parallel and the G' is larger than the G" due to the completion of crosslinking reaction.

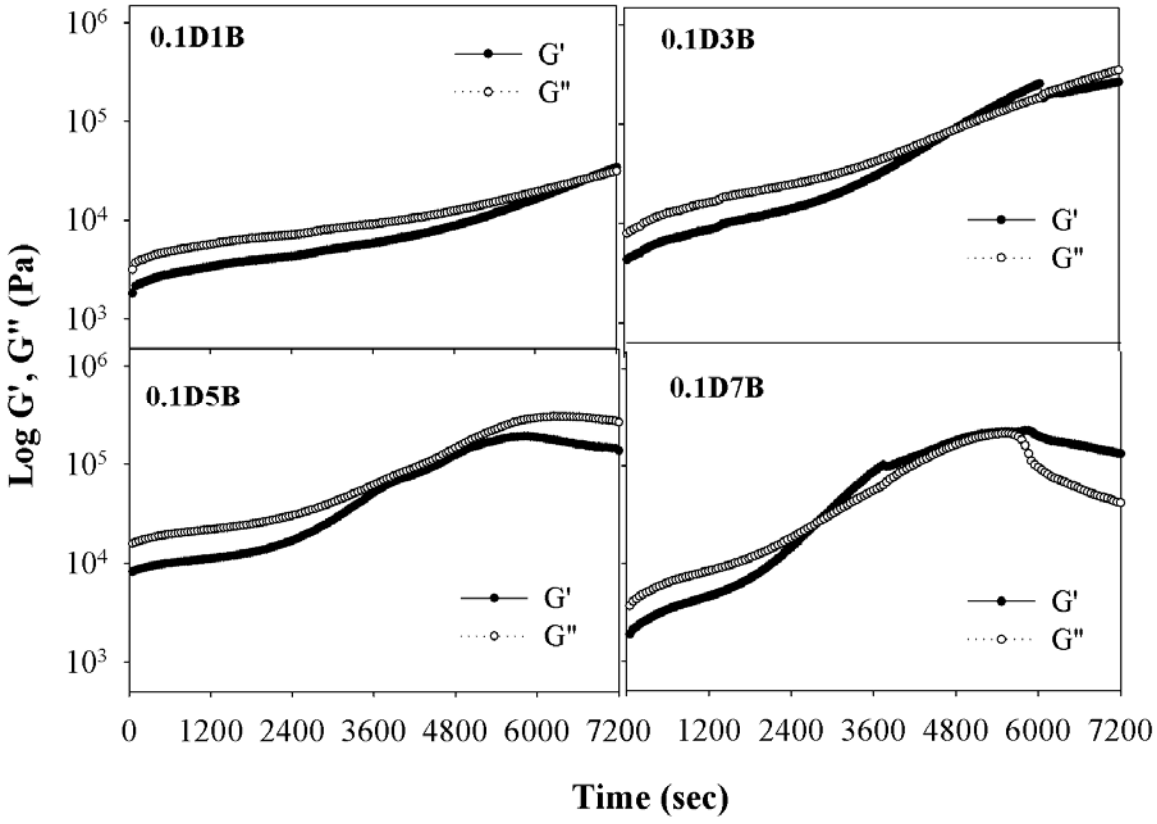

Figure 4.5 G' and G" as a function of time of 0.1DCP/PLA/Bis–EMAs at 150 ºC.

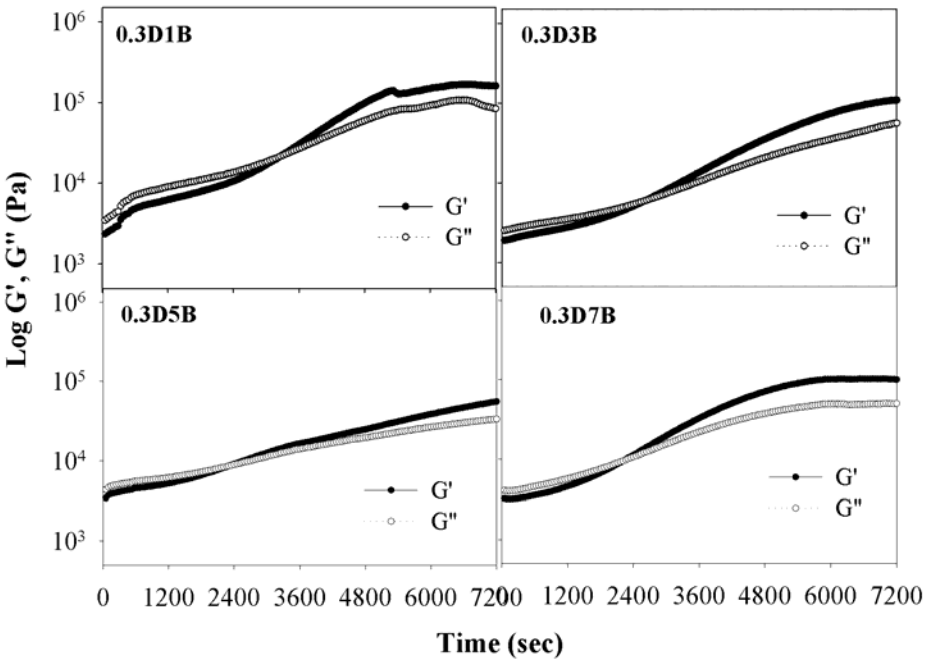

Figure 4.6 G' and G" as a function of time of 0.3DCP/PLA/Bis–EMAs at 150 ºC.

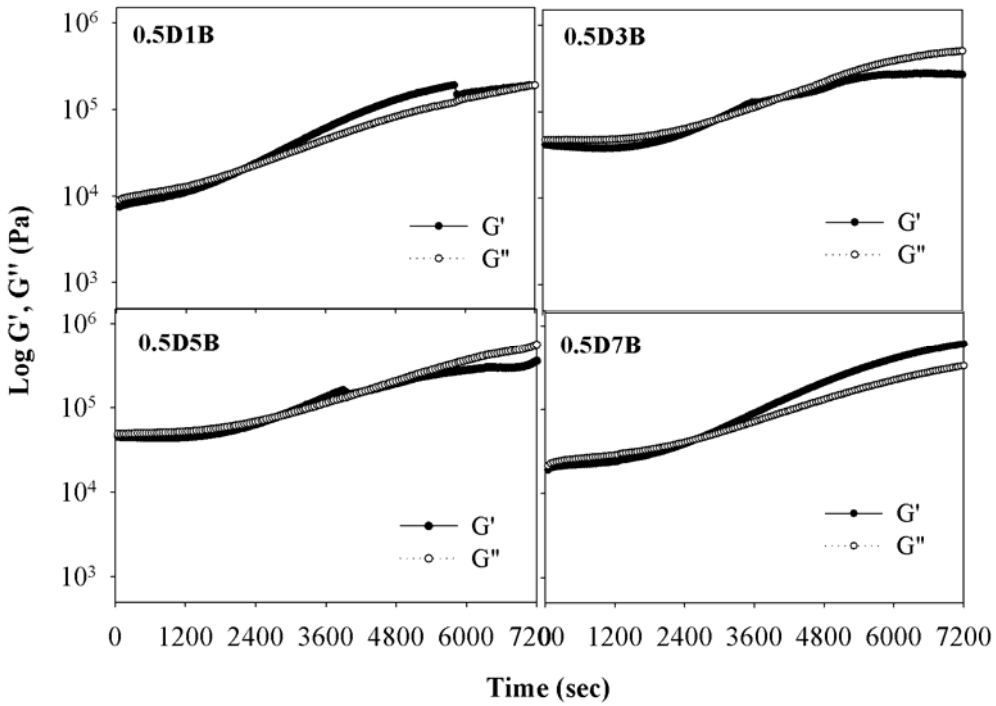

Figure 4.7 G' and G" as a function of time of 0.5DCP/PLA/Bis–EMAs at 150 ºC.

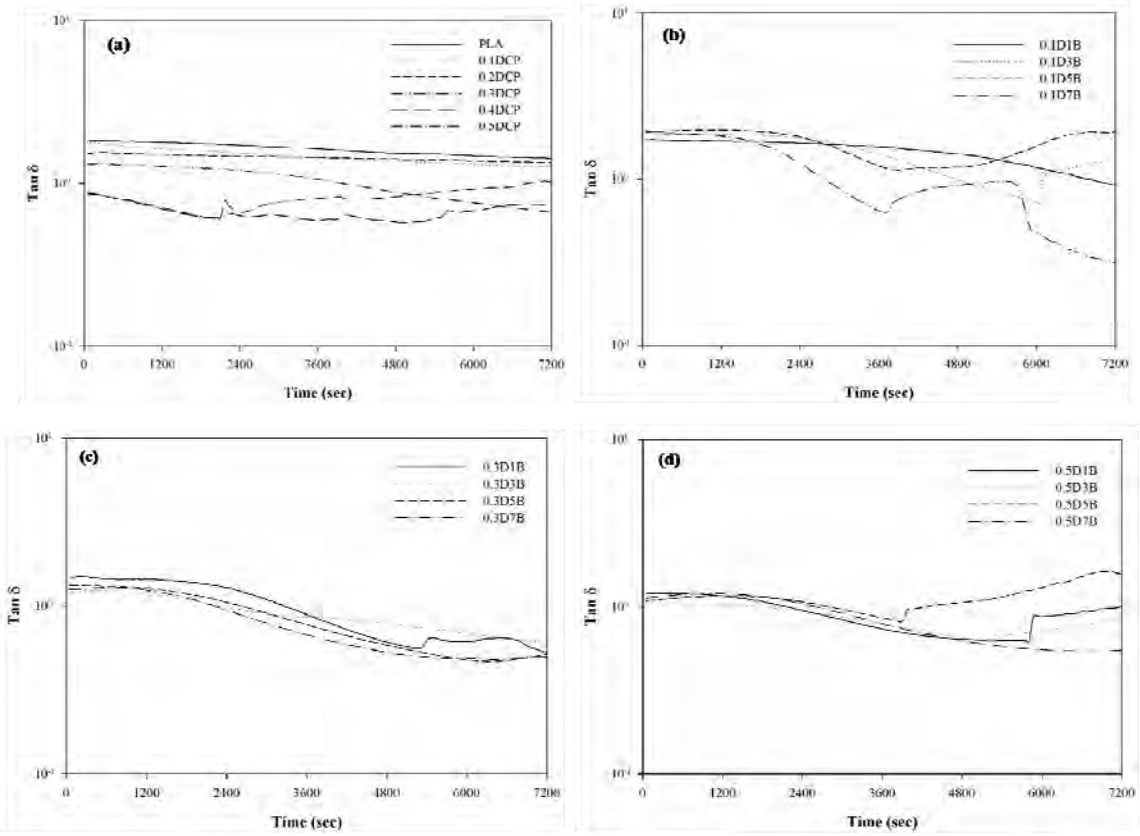

Figure 4.8 Tan δ as a function of time of (a) DCP/PLA, (b) 0.1DCP/PLA/Bis–EMAs, (c) 0.3DCP/PLA/Bis–EMAs, and (d) 0.5DCP/PLA/Bis–EMAs at 150 ºC.

To determine the gel point during a crosslinking reaction of DCP/PLA/Bis–EMAs, the G' and G" are measured as a function of time at 150 °C as shown in Figure 4.5–4.7. At early times, all DCP/PLA/Bis–EMAs show that the elastic portion G' is much smaller than the viscous portion G". The presence of a small elastic contribution well before the critical gel point is due to the stretching of the polymer under deformation and potentially physical entanglements between the polymer chains.

Before gel point, DCP/PLA/Bis–EMAs show lower moduli than PLA. This suggests that DCP/PLA/Bis–EMAs are process easier than PLA. Since the samples before gel point are still in liquid state where viscous properties dominate [28].

As the reactions begin to gel and a crosslinked network is formed, both G′ and G″ begin to increase; however, the rate of increase of G′ is much higher than that of G″ since now the elastic properties dominate. At the gel point, the crossover point between G' and G" values of 0.1DCP/PLA/Bis–EMAs are ~26,300 Pa–93,600 Pa and both G′ and G″ values increase with an increase in Bis–EMAs up to 5 phr as seen in Table 4.1. The moduli values at gel point of 0.3DCP/PLA/Bis–EMAs and 0.5DCP/PLA/Bis–EMAs are ~8,030 Pa–21,500 Pa and ~20,700 Pa–80,200 Pa, respectively. The results of PLA show that the G' (~40,400 Pa–59,100 Pa) and G" (~73,000 Pa–84,200 Pa) are parallel and G">G'. The crossover point between G' and G" values of all DCP/PLA/Bis–EMAs samples decreased when compared to PLA. In the case of 0.3DCP/PLA/Bis–EMAs samples, both G′ and G″ values (~8,030 Pa–21,500 Pa) at gel point are higher than 0.3DCP/PLA (7,670 Pa). This suggests that the addition of Bis–EMAs is effectively crosslink agent to promote crosslinking structure due to improvement in moduli. In the case of 0.5DCP/PLA/Bis–EMAs samples, the addition of Bis–EMAs at 1 phr and 7 phr into 0.5DCP/PLA observes the gel point. Especially 0.5D3B and 0.5D5B samples are not clearly observed the cross over between G' and G" but it is observed the nearest point between G' and G" (at 2980 sec for 0.5D3B and 2730 sec for 0.5D5B). Moreover, 0.5DCP/PLA/Bis–EMAs shows higher the moduli at gel point than 0.3DCP/PLA/Bis–EMAs. This indicates that a large amount of DCP together with Bis–EMAs content obtained high moduli due to a large amount of network structure. At gel point, all DCP/PLA/Bis–EMAs samples are still lower both G′ and G″ than PLA, which means that DCP/PLA/Bis–EMAs is still process easier than PLA.

As the crosslinking reaction progresses, elastic modulus G' is increased due to more entanglements of polymers. Both G′ and G″ values above the gel point of all DCP/PLA/Bis–EMAs samples become higher than PLA. In the case of 0.1DCP/PLA/Bis–EMAs, G" becomes higher than G' after the cross point, which suggests that small amount of crosslinking structure occurred and the sample has more part of viscous properties. For 0.3DCP/PLA/Bis–EMAs, the G' becomes larger than the

G" after gel point. Stiffer gels will have a higher G'. Moreover, 0.5DCP/PLA/Bis–EMAs show the highest moduli values and higher than 0.5DCP/PLA. Especially 0.5D3B and 0.5D5B samples show G">G' over the time period measurement but it has the nearest value between G' and G", which are in the range of 2400 sec–4600 sec as seen in Figure 4.7. This case suggests that the combination of branching and crosslinking reaction can possibly occur.

Figure 4.8(a) shows tan δ which is the ratio of G" to G' or damping of PLA and DCP/PLA. The tan δ reveals that the molecular motion of PLA is greater when compared to DCP/PLA. Tan δ values of 0.1DCP/PLA and 0.2DCP/PLA are clearly above 1, which indicated that G' and G" crossing does not occur in the time period examined. For the 0.3DCP/PLA, the tan δ value is slightly decreased as increase time and the value equal 1 when G'=G" (gel point). In the case of 0.4DCP/PLA and 0.5DCP/PLA, the tan δ values are below 1 due to G'>G" over the time period measurement which is a characteristic of elastic material. Figure 4.8(b)–4.8(c) show tan δ of DCP/PLA/Bis–EMAs samples. Tan δ of DCP/PLA/Bis–EMAs samples are above 1 when G">G' (before gel point) and below 1 when G'>G" (after gel point). This can be noted that the molecular motions of DCP/PLA/Bis–EMAs are restricted with the increasing G'. The tan δ decreased with an increase in Bis–EMAs content. The limited molecular motion in the melt state of DCP/PLA/Bis–EMAs is due to crosslinking structure. So, the network structure provides stronger intermolecular forces and relatively greater resistance to flow. Moreover, the results show that DCP/PLA/Bis–EMAs are lower molecular motions than PLA.

Table 4.1 G' and G" values at gel point of samples

Sample	G'=G" (Pa) at gel point
0.3DCP	7,670
0.1D1B	26,300
0.1D3B	84,300
0.1D5B	93,600
0.1D7B	26,400
0.3D1B	21,500
0.3D3B	8,650
0.3D5B	8,030
0.3D7B	9,930
0.5D1B	20,700
0.5D3B	23,700 (at gel time~2980 sec)
0.5D5B	80,200 (at gel time~2730 sec)
0.5D7B	46,600

Note: 0.5D3B and 0.5D5B use the nearest point between G' and G" to report.

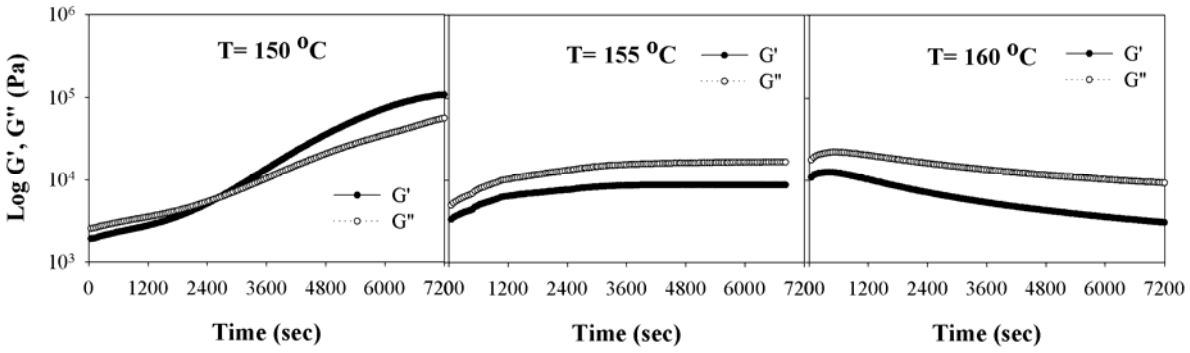

Figure 4.9 G' and G" as a function of time of 0.3D5B at 150 °C, 155 °C, and 160 °C.

Figure 4.9 shows G' and G" of 0.3D5B at various temperature. The results show that temperature at 150 °C has higher moduli (in the range of 10^4–10^5 Pa)

than that of temperature at 155 °C and 160 °C (in the range of 10^3–10^4 Pa). It can be seen that the G' at 150 °C (after 2400 sec) has higher than the G". While the G" become higher than the G' over the time period measurement when increase temperature to 155 °C and 160 °C. This suggests that the sample behaves like a viscous characteristic with increasing temperature. In view of the fact that the moduli are seriously effect on the processing and decrease with an increase temperature. At higher temperature, the connections between molecular chains became weaker because the molecules possessed higher energy than at lower temperature. As a result of this, the melted sample flowed more easily that why the crosslinking sample can process at high temperature.

The gel times of DCP/PLA/Bis–EMAs decreased with increase DCP content as seen in Figure 4.10. The addition of Bis–EMAs shows decrease the gel time of the sample. Moreover, the gel time decreased with the increasing Bis–EMAs content. This confirmed that Bis–EMAs are effectively crosslinking agent to promote crosslinking network of PLA. Moreover, a large amounts of DCP and Bis–EMAs loading show strongly decrease in gel time.

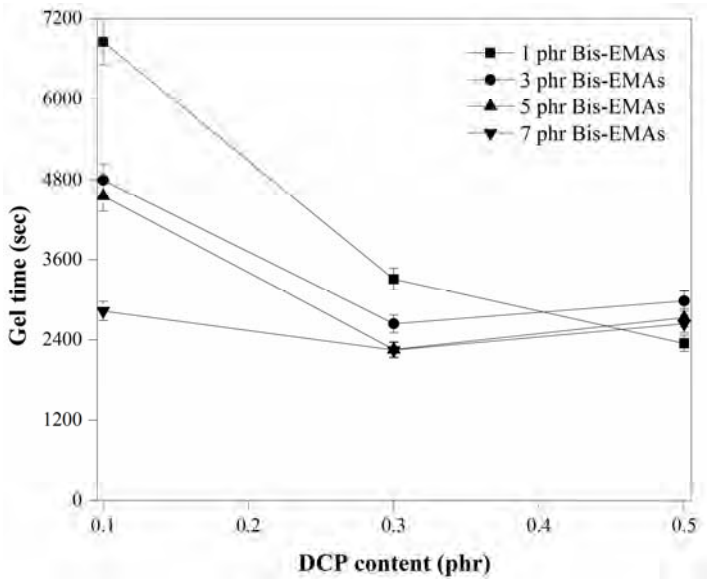

Figure 4.10 Gel time as a function of DCP content at 150 ºC.

4.3.2 Frequency Sweep

The G' of PLA and DCP/PLA as a function of angular frequency at 190 ºC are shown in Figure 4.11(a). At low frequency, the introduction of DCP into PLA more than 3 phr shows increase the G' when compared to PLA. This result suggests that the addition of DCP below 0.3 phr is not sufficient to promote radical for reaction. The G' of DCP/PLA is increased with increasing DCP content. It is well known that DCP can induce crosslinking structure between PLA chains resulted in improve the interaction and entanglement of PLA chain. This result agrees with Huang et al. [29]. They reported that the G' of DCP/PLA increased with DCP content up to 0.5 %wt at low frequency because the incorporation of DCP can be introduced crosslinking structure between PLA chains.

The complex viscosity (η*) of PLA and DCP/PLA as a function of angular frequency at 190 ºC are shown in Figure 4.11(b). The η* of DCP/PLA is increased with increasing DCP content. When compared with PLA, the η* of DCP/PLA decreased when DCP content below 0.4 phr at low frequency. The η* of PLA and DCP/PLA are decreased with increasing frequencies which are a shear thinning behavior or pseudoplastic fluid. Especially 0.4DCP and 0.5DCP are stronger pseudoplastic fluid than PLA.

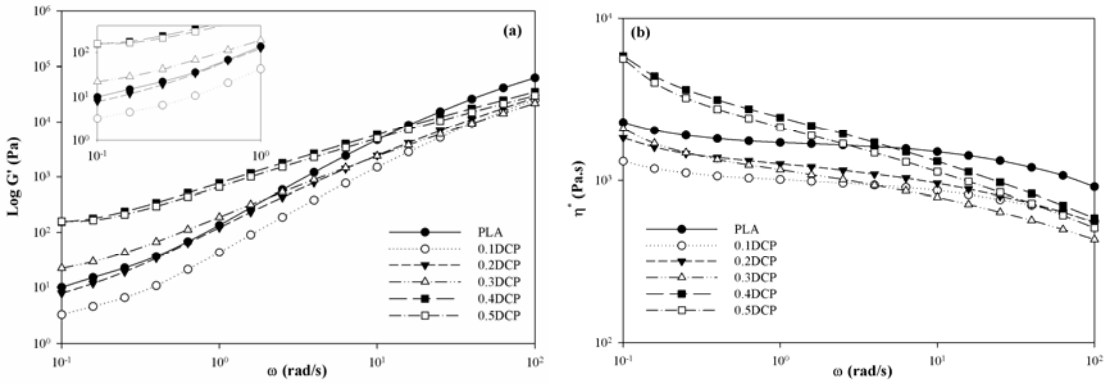

Figure 4.11 Variations of (a) G' and (b) η* as a function of angular frequency at 190 ºC of DCP/PLA.

The G' and η* of PLA and Bis–EMAs/PLA as a function of angular frequency at 190 ºC are shown in Figure 4.12. The G' and η* of Bis–EMAs/PLA are lower than that of PLA. The G' and η* decreased with the increasing Bis–EMAs content, implies that Bis–EMAs was not reacted with PLA chains to form the crosslinking structure, and acted as a role of plasticizer.

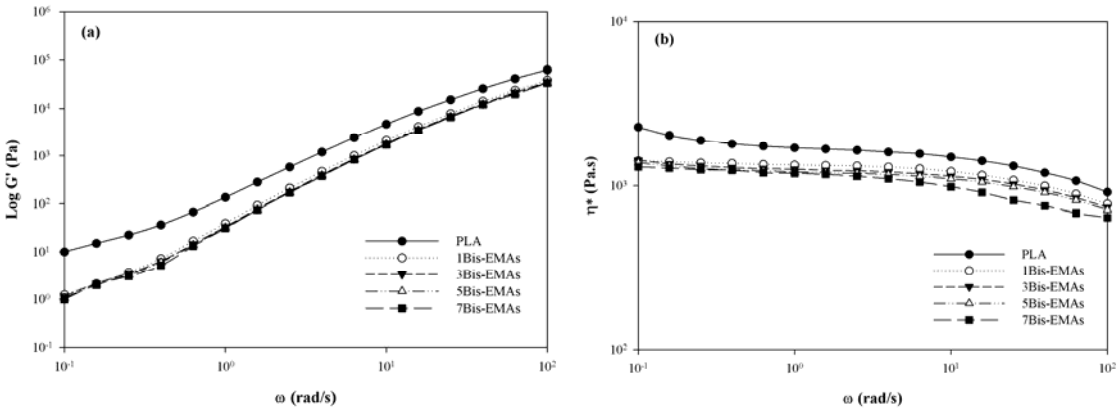

Figure 4.12 Variations of (a) G' and (b) η* as a function of angular frequency at 190 ºC of Bis–EMAs/PLA.

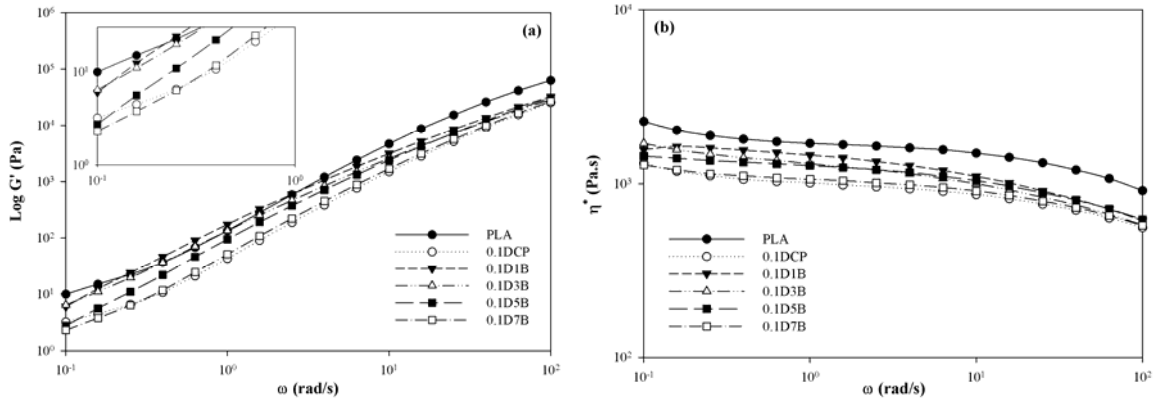

Figure 4.13 Variations of (a) G' and (b) η* as a function of angular frequency at 190 ºC of 0.1DCP/PLA/Bis–EMAs.

Figure 4.13(a) shows the G' of 0.1DCP/PLA/Bis–EMAs. It can be seen that 0.1DCP/PLA/Bis–EMAs show lower the G' than that of PLA. This is due to low amounts of radicals are generated which are not enough to promote crosslinking structure between PLA and Bis–EMAs. When compared to 0.1DCP/PLA, the addition of Bis–EMAs below 5phr increased the G'. As the increasing Bis–EMAs content, the G' is dramatically decreased. Figure 4.13(b) shows that 0.1DCP/PLA/ Bis–EMAs are lower the η* than that of PLA. The η* also decreased with increasing Bis–EMAs content. This case is not suitable reaction for chemical crosslinking PLA with Bis–EMAs.

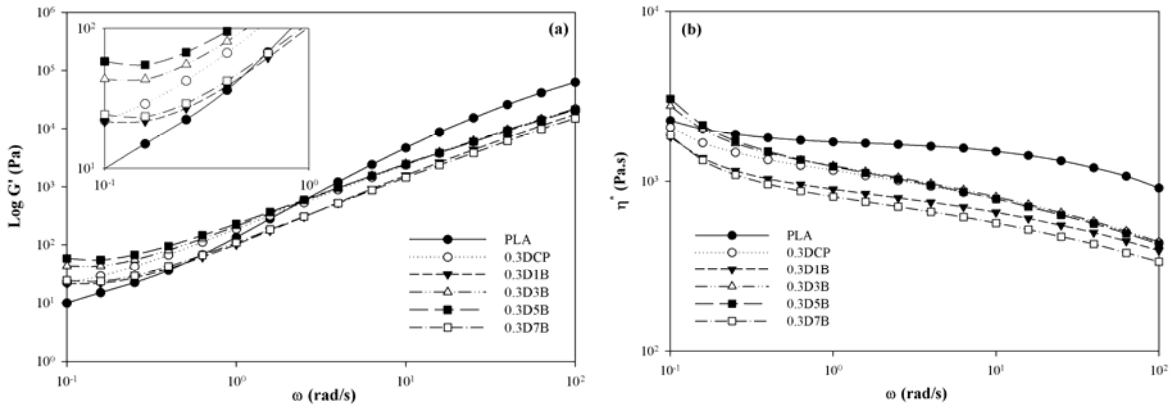

Figure 4.14 Variations of (a) G' and (b) η* as a function of angular frequency at 190 ºC of 0.3DCP/PLA/Bis–EMAs.

In Figure 4.14(a), 0.3DCP/PLA/Bis–EMAs are higher the G' than that of PLA and 0.3DCP/PLA at low frequency. It can be seen that 0.3DCP/PLA/Bis–EMAs showed plateau G' at low frequencies (0.1 rad/s–0.3 rad/s). In the principle, plateau G' is associated with chains entanglement or crosslinking structure in polymer melt [30]. The G' of 0.3DCP/PLA/Bis–EMAs is increased with the addition of Bis–EMAs up to 5 phr. The increasing G' means that enhanced the melt elasticity of material [31]. Further increasing Bis–EMAs over 5 phr resulted in decrease the G'. This result agrees with decrease in gel fraction as seen in Figure 4.10. Consequently, the optimum

of the G' is at 5 phr Bis–EMAs loading and decreases as more Bis–EMAs content. This concludes that the added Bis–EMAs at 5 phr are the best desired crosslinking reaction for 0.3DCP/PLA/Bis–EMAs. As seen in Figure 4.14(b), 0.3DCP/PLA/Bis–EMAs at 3 phr and 5 phr of Bis–EMAs are higher η* than that of PLA and 0.3DCP/PLA at low frequency. The η* of 0.3DCP/PLA/Bis–EMAs is increased with the increasing Bis–EMAs up to 5 phr Bis–EMAs.

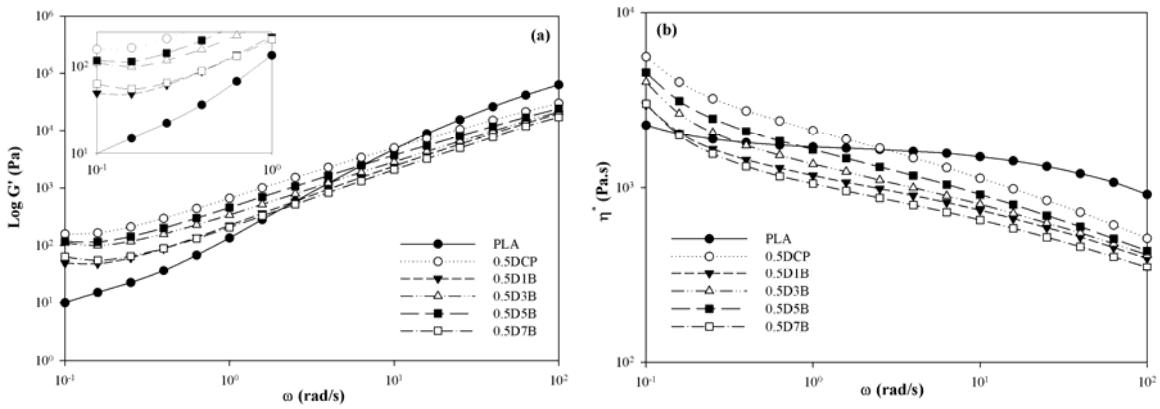

Figure 4.15 Variations of (a) G' and (b) η* as a function of angular frequency at 190 ºC of 0.5DCP/PLA/Bis–EMAs.

In the case of 0.5DCP/PLA with the various amounts of Bis–EMAs are shown in Figure 4.15(a). The results show that the plateau G' of 0.5DCP/PLA/Bis–EMAs is higher than that of PLA but lower than that of 0.5DCP/PLA at low frequency. This can be proposed as two competitive reaction as seen in scheme 4.2. The adding at low amount of crosslinking agent can be created the chain branching while the high amount of crosslinking agent can be created the crosslinking structure [27]. This indicates that the combination of branching and crosslinking structures can be occurred in this case. At low frequency, the plateau G' increased with the increasing Bis–EMAs up to 5 phr and further decreased when Bis–EMAs over 5 phr. The η* of

0.5DCP/PLA/Bis–EMAs shows the tendency in agreement with G' as seen in Figure 4.15(b).

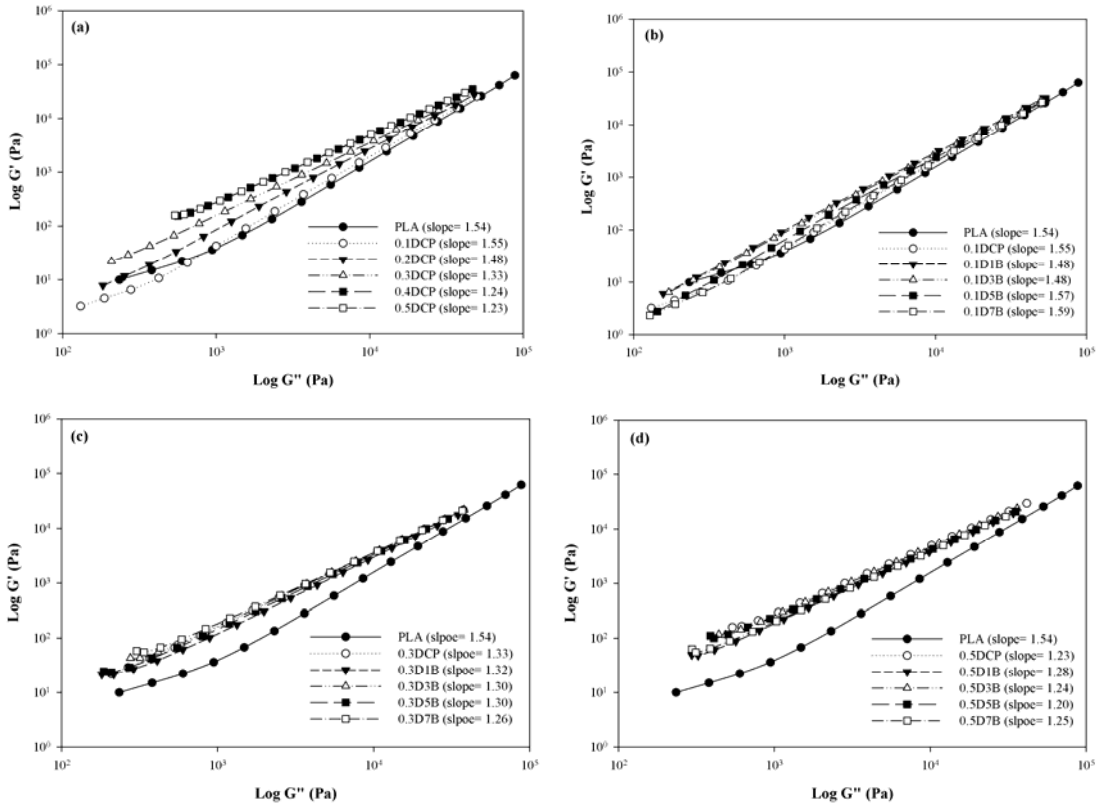

Figure 4.16 Cole–cole plot at 190 ºC of (a) DCP/PLA, (b) 0.1DCP/PLA/Bis–EMAs, (c) 0.3DCP/PLA/Bis–EMAs, and (d) 0.5DCP/PLA/Bis–EMAs.

The Cole–Cole plot or log G' versus log G" as shown in Figure 4.16 can represent the crosslinking, branching, and chain scission. In general, the slope of linear polymer from Cole–Cole plot is about 2 and dependent on the chain branching and crosslinking level [26, 33]. In Figure 4.16(a), the results show that the slopes of DCP/PLA are lower than that of PLA. It can be concluded that the chain structure changes by the formation of crosslinking. As seen in Figure 4.16(b), 0.1DCP/PLA with various Bis–EMAs does not significant change in slope due to a little crosslinking structure. In Figure 4.16(c)–4.16(d), the slopes of crosslinked PLAs decreased with

increasing Bis–EMAs content. Moreover, 0.5DCP/PLA with various Bis–EMAs are lower the slopes than that of 0.3DCP/PLA with various Bis–EMAs. This means that increase in DCP and Bis–EMAs content are significant change the structure of PLA.

4.4 Thermogravimetry

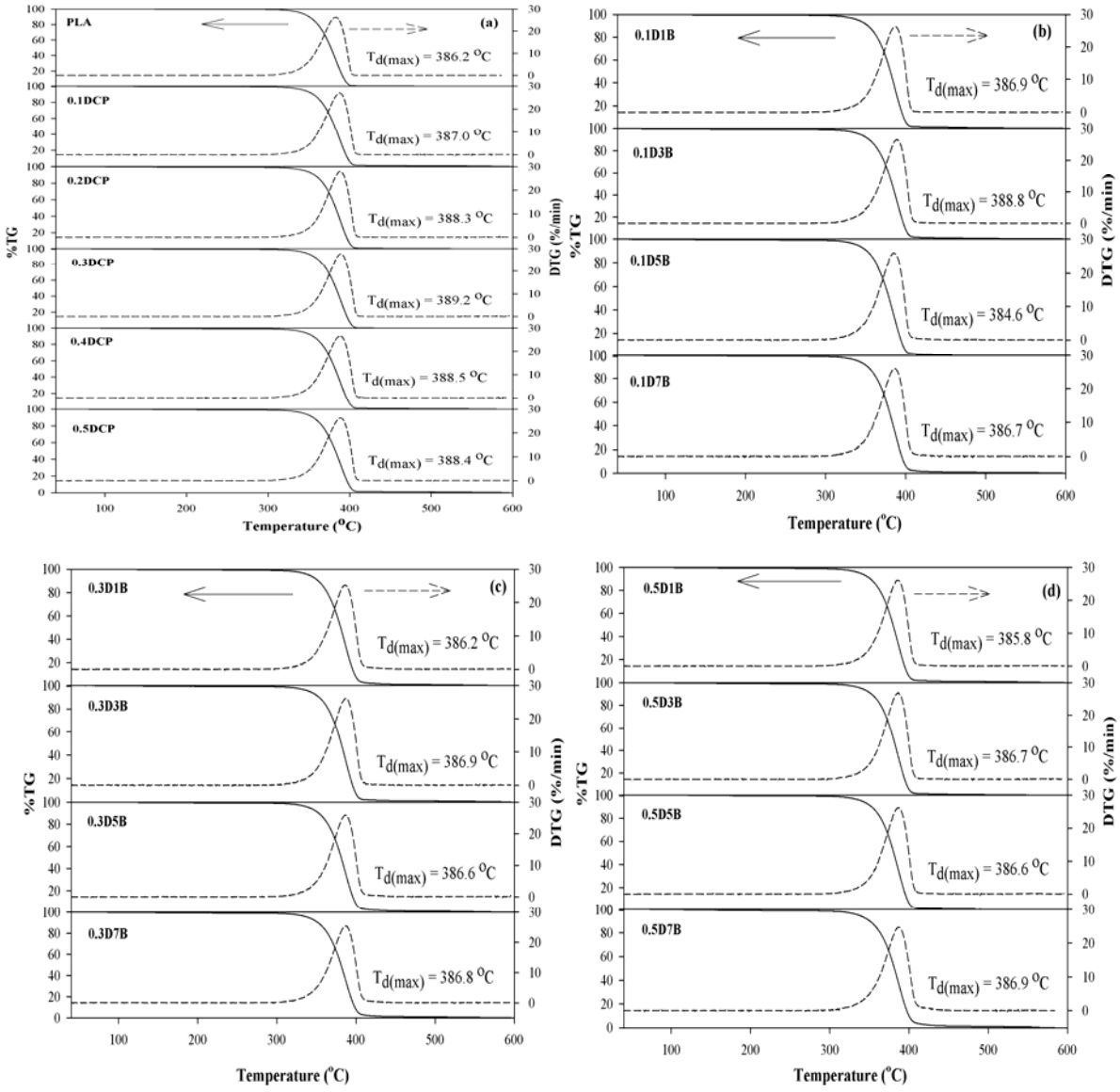

Figure 4.17 TGA thermograms of (a) DCP/PLA, (b) 0.1DCP/PLA/Bis–EMAs, (c) 0.3DCP/PLA/Bis–EMAs, and (d) 0.5DCP/PLA/Bis–EMAs.

Figure 4.17 shows the thermogravimetric (TG) and derivative thermogravimetric (DTG) curves of PLA, DCP/PLA, and DCP/PLA/Bis–EMAs. The decomposition temperature is the temperature at the maximum rate of mass loss ($T_{d(max)}$), or DTG curve. In Figure 4.17(a), the decomposition temperatures of DCP/PLA are slightly higher than that of PLA. This can be ascribed to the introduction of DCP improves the thermal stability of PLA. In addition, the results of DCP/PLA/Bis–EMAs show one transition in its chain decomposition at T_{max}~386.5 °C, which are similarly vales with PLA (T_{max}~386.2 °C) as seen in Figure 4.17(b)–4.17(d). However, the thermal stability of DCP/PLA/Bis–EMAs does not significantly change with increasing Bis–EMAs content.

4.5 Crystallization and Melting Behavior

4.5.1 Thermal Properties of PLA, DCP/PLA, and DCP/PLA/Bis–EMAs Pellets

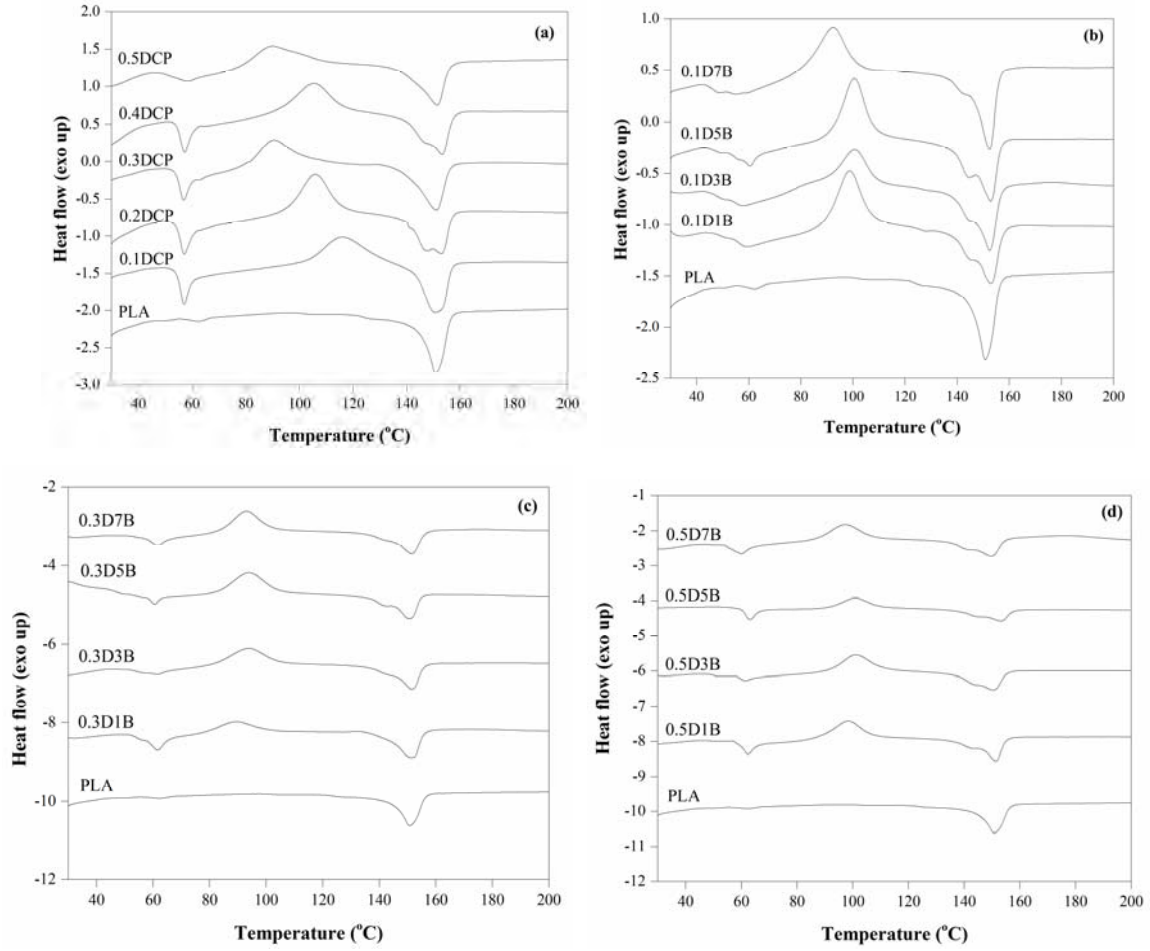

Figure 4.18 DSC thermograms of (a) DCP/PLA, (b) 0.1DCP/PLA/Bis–EMAs, (c) 0.3DCP/PLA/Bis–EMAs, and (d) 0.5DCP/PLA/Bis–EMAs pellets.

Figure 4.18(a) and Table 4.2 show the DSC thermograms of PLA and DCP/PLA. The T_g of DCP/PLA was slightly decreased when compared to PLA. The

T_g and T_{cc} of DCP/PLA decreased with the increasing DCP content. This was due to the generation of high cumyloxy radical can encourage chain scission of PLA as seen in the scheme 4.1 [10].

Figure 4.18(b) shows the DSC thermograms of 0.1DCP/PLA/Bis–EMAs. The results show that 0.1DCP/PLA/Bis–EMAs pellet is lower T_g than that of PLA. This case indicated that a low amount of free radical was generated due to low DCP content. It expected that free Bis–EMAs were not reacted with PLA that can act as a plasticizer in this system. This result agreed with rheological properties of Bis–EMAs/PLA as seen in Figure 4.12. The T_{cc} and T_m of 0.1DCP/PLA/Bis–EMAs decreased with increasing Bis–EMAs content. Moreover, the T_m of 0.1DCP/PLA/Bis–EMAs exhibited two peaks compared to PLA resulted in two kinds of lamellae structure. This explained that the low–melting peak corresponding to less perfect crystal structure while the high–melting peak corresponding to more perfect crystal structure [33]. So, this case was not suitable to produce the crosslinking PLA.

Figure 4.18(c) and 4.18(b) show the DSC thermograms of 0.3DCP/PLA/Bis–EMAs and 0.5DCP/PLA/Bis–EMAs, respectively. The results demonstrated that T_g of both samples were slightly higher than PLA. It suggested that crosslinking structure decreased chain motion. The T_{cc} of both samples were shift to higher temperature with increase in Bis–EMAs content. This explained that a large molecular chain networks inhibited chain segment motion for crystallization. T_m of both samples did not change when compared to PLA.

The crystallinities of DCP/PLA/Bis–EMAs decreased when compared to PLA. Moreover, high amounts of DCP together with Bis–EMAs contents promoted a large crosslinking structure resulted in decreasing crystallinity, which obstructed the PLA chains for crystallization.

Table 4.2 Thermal properties of PLA, DCP/PLA, and PLA/DCP/Bis–EMAs pellets

Sample	**T_g (˚C)**	**T_{cc} (˚C)**	**ΔH_{cc} (J/g)**	**T_{m1}; T_{m2} (˚C)**	**ΔH_m (J/g)**	**χ_c (%)**
PLA	57.9	-	-	151.2	44.8	48.1
0.1DCP	55.5	115.6	31.2	151.9	41.9	11.5
0.2DCP	55.4	105.9	36.7	152.9	45.0	8.9
0.3DCP	55.1	90.2	29.9	151.2	40.9	11.8
0.4DCP	55.5	105.3	33.0	152.5	41.7	9.3
0.5DCP	54.7	88.5	32.2	151.6	41.5	10.0
0.1D1B	56.5	98.6	33.4	144.7: 153.1	41.6	8.8
0.1D3B	55.4	100.8	30.6	143.6: 152.8	41.7	11.9
0.1D5B	54.4	100.5	33.5	144.3: 153.2	43.4	10.6
0.1D7B	45.5	92.5	36.8	142.8: 152.6	46.3	10.2
0.3D1B	58.4	89.2	30.2	151.9	40.6	11.1
0.3D3B	58.1	93.7	37.3	152.1	42.8	5.9
0.3D5B	59.5	93.8	38.7	151.1	39.9	1.1
0.3D7B	59.3	93.0	38.8	151.7	41.3	2.6
0.5D1B	60.5	98.4	38.2	151.5	42.1	4.1
0.5D3B	59.2	100.9	38.5	150.8	43.3	5.1
0.5D5B	60.7	101.0	38.5	151.5	40.4	2.0
0.5D7B	58.4	97.0	35.7	150.1	41.9	6.6

4.5.2 Thermal Properties of 0.3D5B Sample from Compression Molding

In the case of varying time for compression molding, the results at 180 ºC show that the T_g of sample decreased with increasing compression time as seen in Figure 4.19. Similar to T_g, T_{cc} and T_m also reduced with increasing compression time. This suggests that PLA chains degraded with increasing compression time. Increasing temperature to 190 ºC, PLA chains clearly degraded further so that its T_g, T_{cc} and T_m decreased more. The cold crystallization temperature is typically changed similarly to

T_g. However, it was found that T_g at temperature of 200 ºC became higher than that at 190 ºC even at 2.5 min of compresstion time. The highest T_g was at 200 ºC for 5 min as seen in Figure 4.19. This suggests that this high temperature causes not only the degradation to PLA chains but also the decrease in viscosity of all components and so the degraded chains can easily react to the free Bis-GMA bringing more densely crosslinking which contributed to an increase in T_g and less crystallinity, see Table 4.3. This condition thus minimized the reduction in the thermal properties of the sample except crystallinity. However, further increasing compression time the PLA chain degradation turned to be dominant. Moreover, T_m of the sample exhibited two peaks (Figure 4.20) revealing the imperfect crystals of the lower T_m component could be a result of the degraded chains. It should be noted that the higher T_m was not changed significantly with increasing temperature and compression time (Table 4.3). So, the temperature and time are important factors for compression or processing condition because PLA chain is sensitive to heat.

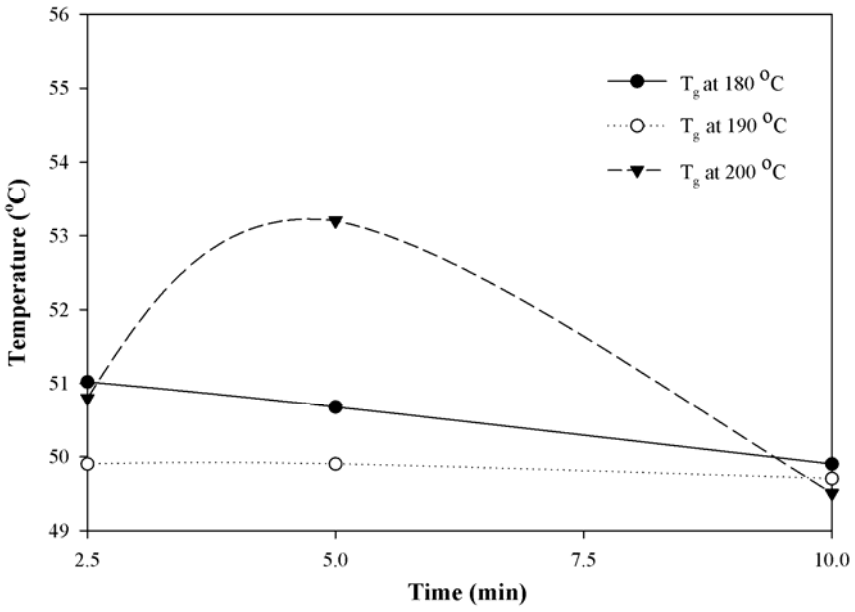

Figure 4.19 The plot of T_g of 0.3D5B sample from compression molding at various temperatures and time.

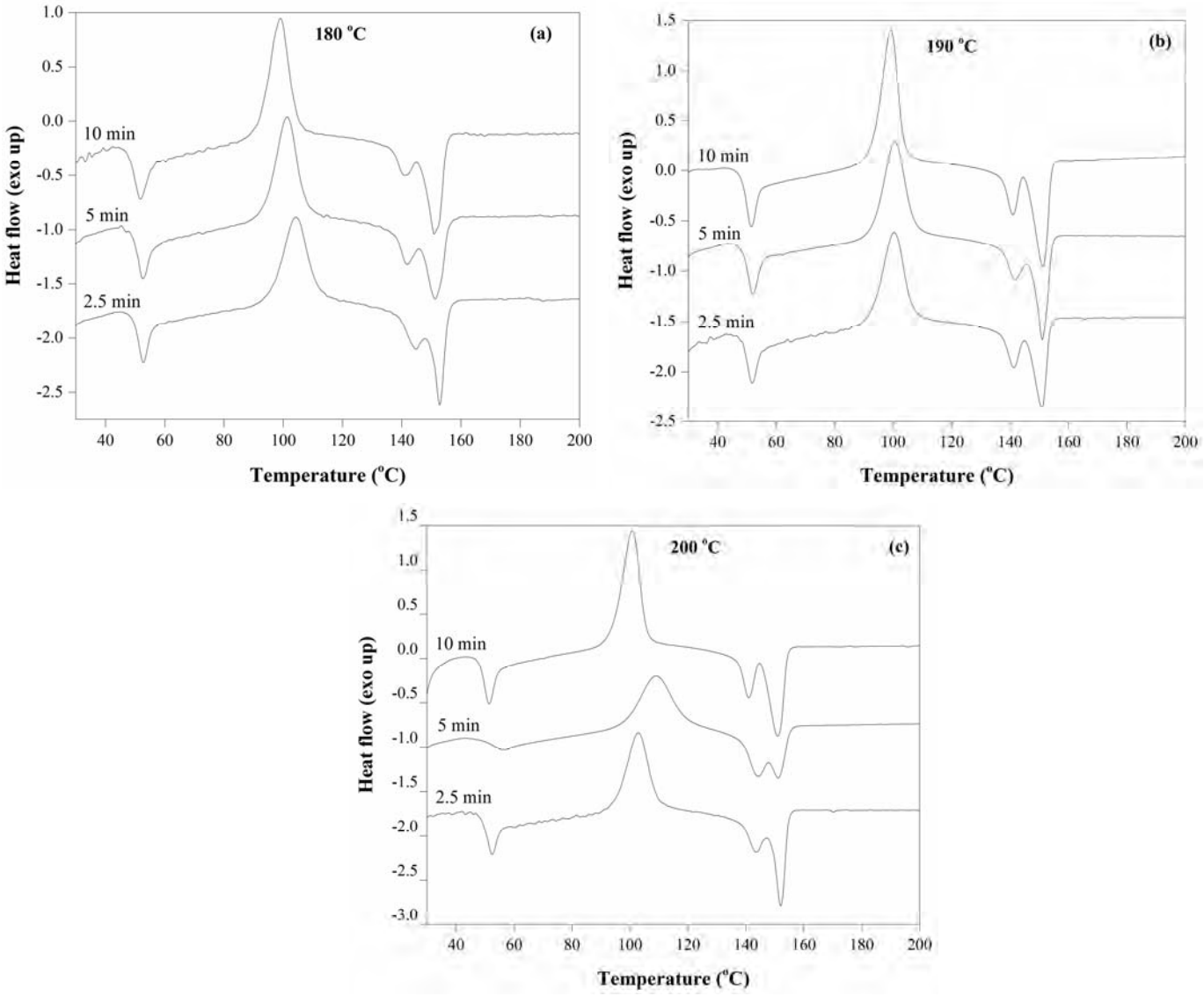

Figure 4.20 DSC thermograms of 0.3D5B sample of (a) 180 ºC, (b) 190 ºC, and (c) 200 ºC.

Table 4.3 Thermal properties of 0.3D5B sample from compression molding at various condition

Condition of compression molding	T_g (˚C)	T_{cc} (˚C)	ΔH_{cc} (J/g)	T_{m1}; T_{m2} (˚C)	ΔH_m (J/g)	χ_c (%)
180 ºC for 2.5 min	51.0	104.3	45.3	144.5: 152.9	48.1	3.0
180 ºC for 5 min	50.7	101.4	45.4	141.6: 151.1	47.4	2.2
180 ºC for 10 min	49.5	98.7	48.4	141.0: 152.1	50.7	2.5
190 ºC for 2.5 min	49.9	100.5	46.1	141.3: 151.2	47.8	1.8
190 ºC for 5 min	49.9	100.6	51.6	141.4: 151.1	53.4	1.9
190 ºC for 10 min	49.7	99.2	56.7	141.0: 151.5	57.9	1.3
200 ºC for 2.5 min	50.8	103.0	46.0	143.5: 152.3	47.9	2.0
200 ºC for 5 min	53.2	109.0	44.9	144.2: 151.2	46.3	1.5
200 ºC for 10 min	49.5	100.9	57.2	141.0: 151.2	58.4	1.3

4.6 Mechanical properties

Mechanical properties of PLA and crosslinked PLA samples are shown in Figure 4.21 and Table 4.4. The introductions of DCP and Bis–EMAs into PLA result to an increase in Young's modulus and a decrease of elongation at break. This suggests that PLA material was stiffened when crosslink structure was introduced to PLA. In the case of 0.3DCP/PLA/Bis–EMAs, the tensile strength firstly increases and then decreases with increasing Bis–EMAs content up to 7 phr. It can be seen that the highest tensile strength is obtained from 0.3D5B sample. Moreover, at the same introductions of Bis–EMAs contents, which are 0.3D7B and 0.5D7B samples, do not significantly changes of tensile strength and Young's modulus values. From these results, it could be noted that the optimums of tensile strength and Young's modulus were at a 5 phr Bis–EMAs.

Impact strength of PLA and crosslinked PLA is shown in Table 4.4. Impact strength of crosslinked PLA slightly decreased when compared to PLA. This

suggests that crosslinked PLA has higher rigidity than PLA due to network structure. Moreover, it can be seen that impact strength of 0.3DCP/PLA/Bis–EMAs decreases with increasing Bis–EMAs content up to 5 phr where the strongest crosslinked structure and rigidity was formed. The lowest impact strength is also obtained from 0.3D5B.

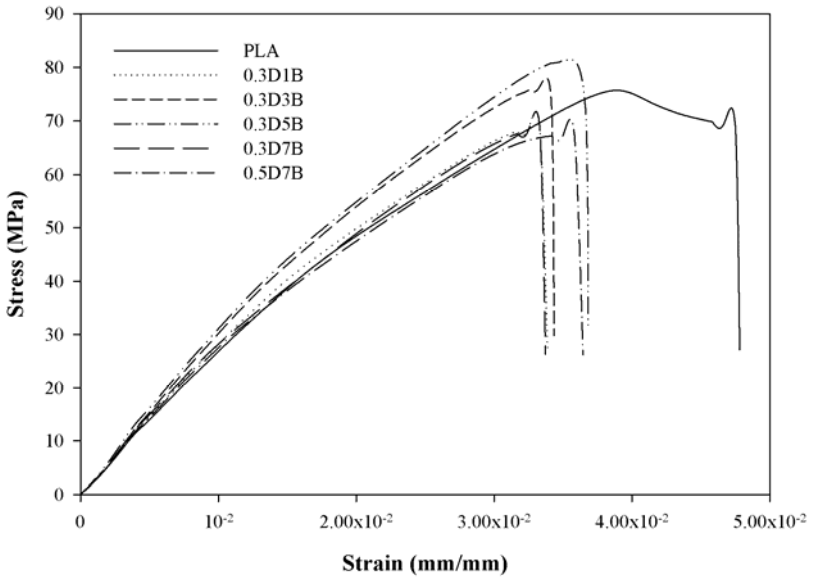

Figure 4.21 Stress–strain curves of PLA, 0.3D1B, 0.3D3B, 0.3D5B, 0.3D7B, and 0.5D7B samples.

Table 4.**4** Mechanical properties of PLA, 0.3D1B, 0.3D3B, 0.3D5B, 0.3D7B, and 0.5D7B

Sample	**Tensile strength (MPa)**	**Young's modulus (MPa)**	**Elongation at break (%)**	**Impact strength (J/m)**
PLA	66.15±7.46	2681.98±156.61	5.00±0.30	55.10±1.20
0.3D1B	67.54±5.29	3155.40±179.15	3.00±0.40	55.10±1.00
0.3D3B	69.51±3.54	3343.79±147.81	3.00±0.20	51.30±2.50
0.3D5B	72.62±1.89	3453.64±75.30	4.00±0.20	47.50±1.20
0.3D7B	65.70±4.50	3196.24±144.56	3.00±0.30	51.30±1.50
0.5D7B	64.21±4.22	3084.17±114.96	4.00±0.30	52.50±1.40

4.7 Thermo−Mechanical Properties

Figure 4.22(a) and Table 4.5 show the effect of temperature on storage modulus (E'), which relates directly to the stiffness of materials. At ambient temperature, E' of DCP/PLA is higher than that of PLA. It can be seen that E' of DCP/PLA also increased with the increasing DCP content because the crosslinking improved the modulus of the material. In the case of DCP/PLA/Bis–EMAs as seen in Figure 4.23(a)–4.25(a), the E' increased with increasing Bis–EMAs up to 5 phr.

In the glass transition region, the E' of all samples is decreased. When the temperature is higher than T_g, the E' of all samples shows an abrupt increase which is attributed to cold crystallization. At temperature higher (>100 ºC), DCP/PLA and DCP/PLA/Bis–EMAs have higher E' than that of PLA. This means that DCP/PLA and DCP/PLA/Bis–EMAs can bear loads at higher temperatures better than that of PLA because the development of rigidity is a result of the cold crystallization. At 120 ºC, DCP/PLA and DCP/PLA/Bis–EMAs still show greater rigidity when compared to PLA. This can be noted that crosslinking structures can bear load at temperature beyond the glass transition region.

Figure 4.22(b) and Table 4.5 show the loss modulus (E"), or ability of the material to dissipate energy, which is related to viscosity. DCP/PLA shows higher peak magnitude of the E" when compared to PLA. The E" of DCP/PLA slightly increased with increasing DCP content. This suggests that the addition of DCP improved the viscosity of PLA [34]. In Figure 4.23(b)–4.25(b), the E" peak of DCP/PLA/Bis–EMAs slightly increased with increasing Bis–EMAs content. This can be attributed to the crosslinking structure lead to promote high viscosity. The ratio of E" to E' is measured as a loss factor, or tan δ, as observed in Figure 4.23(a)–4.25(a) and Table 4.5. Damping reveals that the molecular motion of PLA is greater when compared to DCP/PLA/Bis–EMAs. The limited molecular motion in DCP/PLA/Bis–EMAs agrees well to the stiffness due to crosslinking structure.

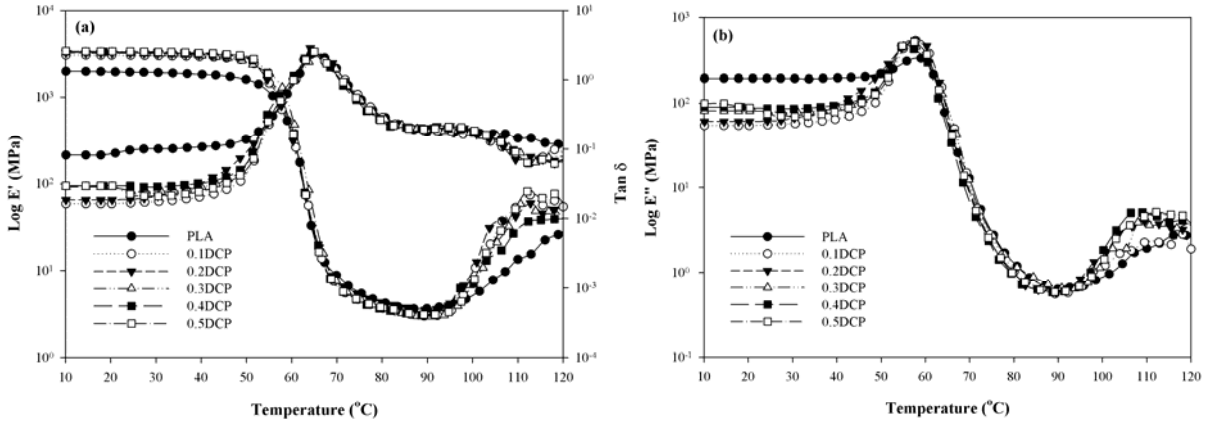

Figure 4.22 Temperature dependence of (a) E' and tan δ, and (b) E'' of PLA and DCP/PLA.

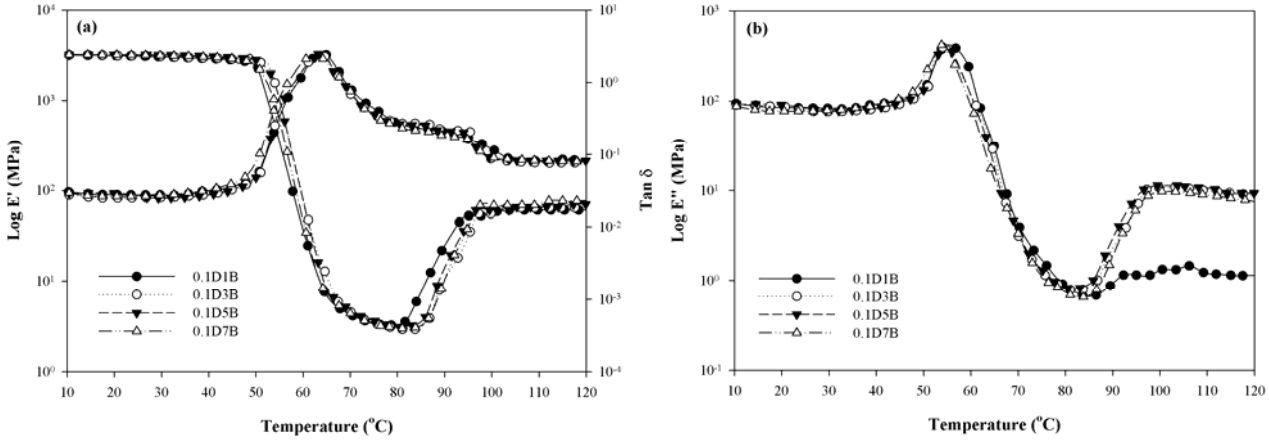

Figure 4.23 Temperature dependence of (a) E' and tan δ, and (b) E'' of 0.1DCP/PLA/Bis–EMAs content.

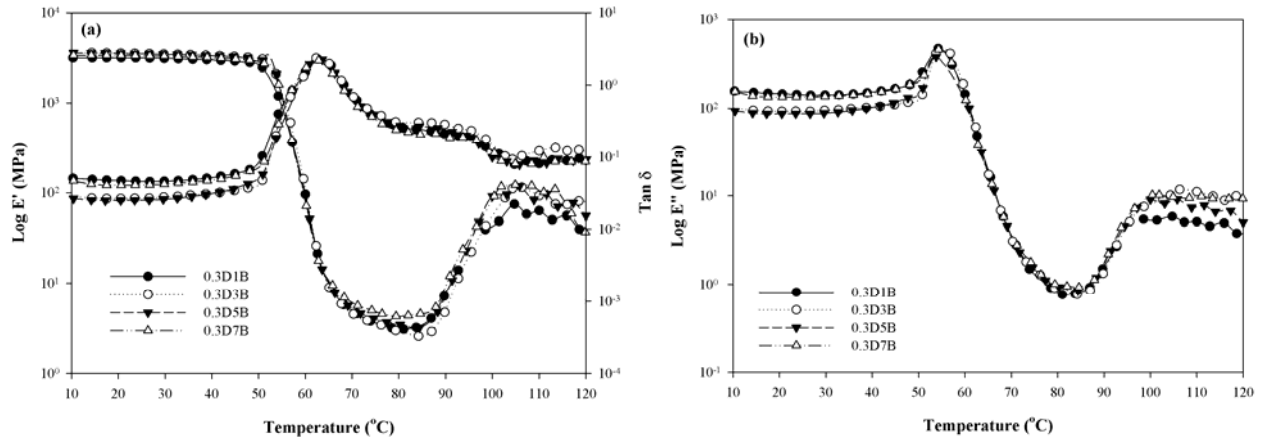

Figure 4.24 Temperature dependence of (a) E' and tan δ, and (b) E'' of 0.3DCP/PLA/Bis–EMAs.

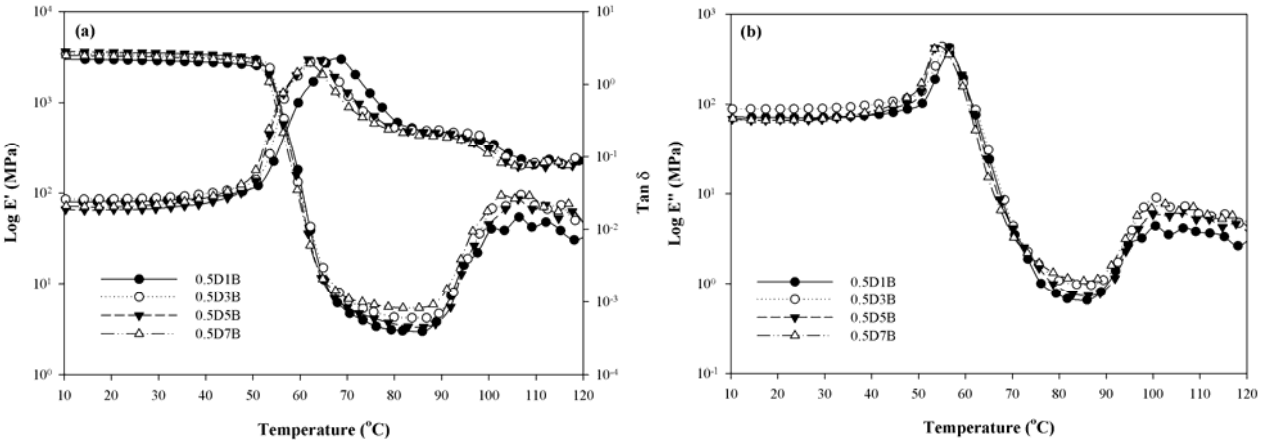

Figure 4.25 Temperature dependence of (a) E' and tan δ, and (b) E'' of 0.5DCP/PLA/Bis–EMAs content.

Table 4.5 Themo–mechanical properties of PLA, DCP/PLA, and DCP/PLA/Bis–EMAs

Sample	T_g (˚C) from Tanδ	30 ˚C		80 ˚C		100 ˚C		120 ˚C	
		E' (MPa)	E"(MPa)	E' (MPa)	E"(MPa)	E' (MPa)	E" (MPa)	E' (MPa)	E"(MPa)
PLA	64.3	1925.04±40.32	193.00±12.95	4.21±0.84	1.19±0.01	5.74±1.02	0.96±0.21	31.72±6.03	3.27±1.06
0.1DCP	64.6	3021.09±56.29	57.14±10.06	2.70±0.03	0.63±0.01	10.77±2.11	1.21±0.43	54.16±5.11	1.90±0.59
0.2DCP	64.1	3199.53±38.01	66.85±8.43	2.41±0.11	1.22±0.04	12.56±1.04	1.76±0.69	43.95±5.86	2.40±0.67
0.3DCP	64.0	3219.72±49.75	77.48±9.12	2.69±0.04	1.02±0.05	10.04±1.90	1.13±0.08	52.11±6.03	3.86±0.41
0.4DCP	64.4	3257.51±62.05	85.69±7.05	2.56±0.14	0.68±0.04	7.07±0.98	1.84±0.14	40.00±2.49	3.38±0.48
0.5DCP	64.9	3322.11±50.30	69.49±8.21	2.41±0.16	0.72±0.01	7.92±2.32	1.44±0.60	54.36±5.92	3.61±0.52
0.1D1B	64.9	3084.15±48.56	81.56±10.23	3.56±0.02	0.91±0.03	52.81±6.09	2.53±0.45	60.79±9.39	2.53±0.68
0.1D3B	64.6	3105.07±83.48	86.05±9.40	2.93±0.03	0.78±0.06	55.55±9.42	9.42±2.59	64.37±11.94	9.23±0.21
0.1D5B	63.2	3185.93±29.54	81.32±8.52	3.11±0.03	0.81±0.02	60.71±11.56	9.05±1.38	70.00±9.02	8.84±1.11
0.1D7B	60.6	3160.29±31.93	76.49±6.59	3.00±0.05	0.68±0.08	68.69±6.52	8.30±2.09	76.85±9.35	8.24±0.85
0.3D1B	62.6	3100.15±40.54	141.22±9.63	3.07±0.05	0.76±0.09	48.53±3.21	5.32±1.02	42.95±5.39	3.89±0.72
0.3D3B	62.3	3461.30±47.58	94.79±7.76	2.96±0.09	0.90±0.02	43.33±2.09	8.99±1.53	77.91±10.38	8.73±0.68
0.3D5B	63.6	3475.32±53.40	87.98±5.69	3.44±0.17	0.93±0.01	91.66±5.28	9.06±1.20	55.89±7.93	5.01±0.42
0.3D7B	62.8	3283.17±50.28	135.54±11.60	4.26±0.03	1.00±0.02	90.99±3.95	10.22±3.29	36.94±3.50	9.29±1.08
0.5D1B	68.7	2889.69±39.59	71.23±9.54	3.09±0.05	0.77±0.02	40.24±2.11	4.45±0.43	34.05±4.02	3.17±0.92
0.5D3B	64.9	3321.82±47.80	89.43±8.59	4.26±0.08	1.08±0.01	67.40±8.42	9.06±1.30	61.04±7.49	5.39±0.47
0.5D5B	61.7	3503.96±41.05	67.41±8.90	3.71±0.03	0.99±0.01	45.42±4.65	5.86±1.04	40.31±5.03	3.49±0.21
0.5D7B	62.1	3175.07±39.46	69.01±5.62	5.37±0.04	1.32±0.04	62.57±5.04	6.88±1.22	46.89±4.60	4.42±0.19

4.8 Morphological Properties

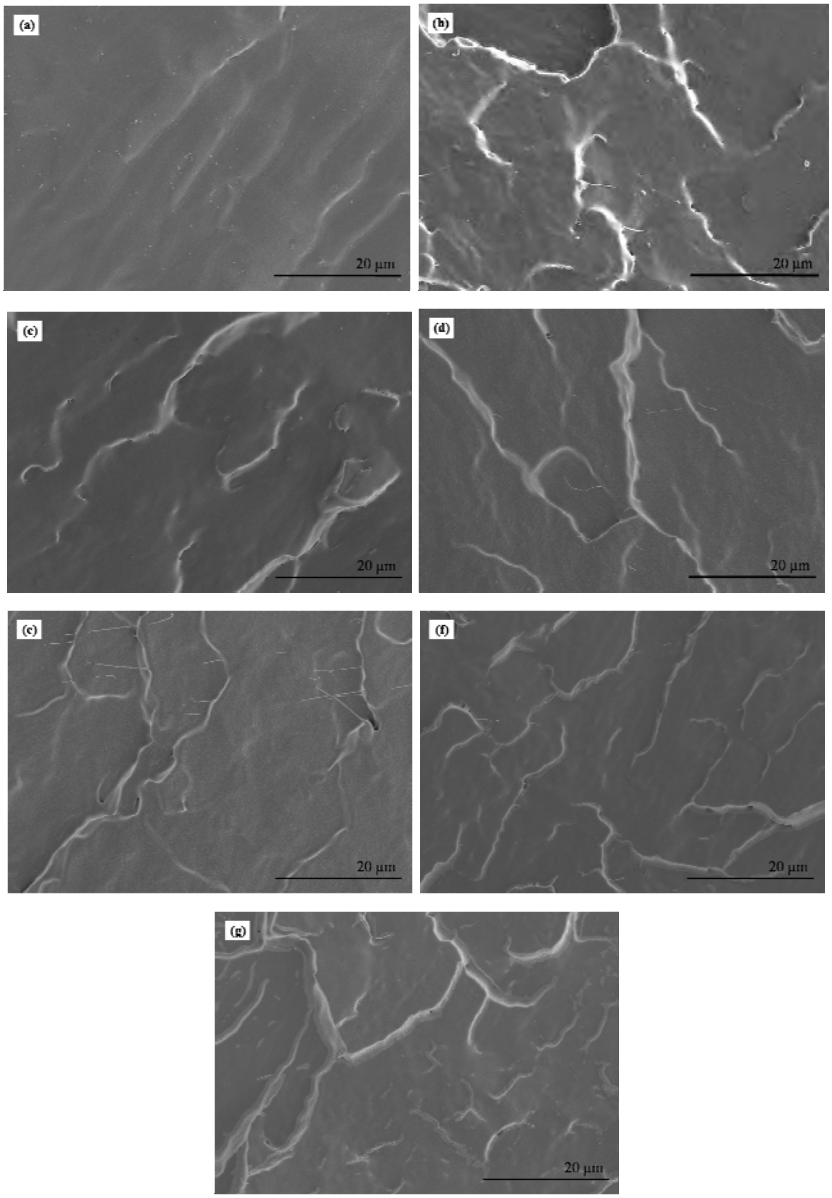

Figure 4.26 Morphological images of (a) PLA, (b) 0.1D1B, (c) 0.1D5B, (d) 0.3D1B, (e) 0.3D5B, (f) 0.5D1B, and (g) 0.5D5B.

The morphology of PLA reveals a smooth and uniform fractured surface as seen in Figure 4.26(a). However, DCP/PLA/Bis–EMAs show rough surface which is observed in Figure 4.26(b)–4.26(g). This can be suggested that the chains entanglement of crosslinking structure is strongly interaction between PLA chains so that the crosslink junctions become stronger and thus retard the breaking or divert the crack growth leading to promote rough surface. Moreover, the fracture surface is rougher when increasing Bis–EMAs content.

In addition, the biodegradation of crosslinked PLA must be further studied. Mitomo et al. [5] studied the biodegradation rate of crosslinked PLA by irradiation. They found that the biodegradation was significantly delayed with the introduction of crosslink because of suppressing the penetrating of microorganisms into polymer gels and increased with increasing irradiation dose due to degradation of crosslinked molecules. This results also found in Quynh et al. [24]. In this work, it may be suggested that DCP/PLA samples have higher biodegradation rate than that of PLA because this system occur some chain scission. In the case of DCP/PLA/Bis–EMAs, the biodegradation of this system may decrease when compared to PLA. This suggests that crosslinked PLA was successfully produced in the presence of Bis–EMAs which retards the degradation.

5. Conclusions and Recommendations

5.1 Conclusions

This work reveals that crosslinking structures can be introduced into PLA by the initiation of DCP in the presence of Bis−EMAs. The rheological properties showed that DCP/PLA revealed the enhancement of G' and η* when added DCP over 0.3 phr. In the case of DCP/PLA/Bis–EMAs, the G' and η* of 0.1DCP/PLA/Bis–EMAs were decreased when compared to PLA because the introduction of 0.1 phr DCP did not enough to generate radicals of PLA chains to react with Bis−EMAs. This case was unfavorable for crosslinking reaction of PLA in the presence of Bis−EMAs. In addition, 0.3DCP/PLA/Bis–EMAs and 0.5DCP/PLA/Bis–EMAs revealed improvement in G' and η* due to effectively introduced crosslinking structure. The optimums of G' and η* were at a 5 phr Bis–EMAs. TGA results revealed that DCP/PLA gave the strucuture with better thermal stability when compared to PLA. The thermal stability of DCP/PLA/Bis–EMAs did not significantly change with increasing Bis–EMAs content. DSC results demonstrated that T_g, T_{cc}, and T_m of DCP/PLA slightly shifted to lower temperature when compared to PLA. The thermal properties of 0.1DCP/PLA/Bis–EMAs decreased with increasing Bis–EMAs content. In the case of 0.3DCP/PLA/Bis–EMAs and 05DCP/PLA/Bis–EMAs, T_g and T_{cc} were increased when compared to PLA because the crosslinking structure inhibited chain motion. The tensile strength and Young's modulus of 0.3DCP/PLA/Bis–EMAs were increased while the impact strength of 0.3DCP/PLA/Bis–EMAs was decreased with increasing Bis–EMAs up to 5 phr. The thermo–mechanical properties showed that the E' and E" of DCP/PLA were higher than that of PLA. In the case of DCP/PLA/Bis–EMAs, the E' and E" increased with increasing Bis–EMAs up to 5 phr. The morphology properties of DCP/PLA/Bis–EMAs showed rough surface due to the chains entanglement of crosslinking structure. This work concluded that the chemical crosslinked PLA was successfully produced in the presence of Bis–EMAs at 5 phr with the introduction of DCP over 0.3 phr.

5.2 Recommendations

The recommendation of the future work will be based:

- Study the biodegradable properties of crosslinking PLA.
- Study the processing condition of crosslinking PLA, such as screw speed or reaction time, and temperature in order to find the optimum condition of crosslinking PLA for processing.

6. References

[1] Satyanarayana, K.G., Arizaga, G.G.C., and Wypych, F. (2009) Biodegradable composites based on lignocellulosic fibers—An overview. Progress in Polymer Science, 34, 982–1021.

[2] Yang, S.L., Wu, Z.H., Meng, B., and Yang, W. (2009) The Effects of Dioctyl Phthalate Plasticization on the Morphology and Thermal, Mechanical, and Rheological Properties of Chemical Crosslinked Polylactide. Journal of Polymer Science: Part B: Polymer Physics, 47, 1136–1145.

[3] Ogliari, F.A., Caroline, E., Cesar, H.Z., Carmen, B.B.F., Susana, M.W.S., Fla´ vio, F.D., Cesar, L.P., Evandro, Piva. (2008) Influence of chain extender length of aromatic dimethacrylates on polymer network development. Dental Materials, 24, 165–171.

[4] Mitomo, H., Kaneda, A., Quynh, T.M., Nagasawa, N., Yoshii, F. (2005) Improvement of heat stability of poly(L-lactic acid) by radiation-induced crosslinking. Polymer, 46, 4695-4703.

[5] Quynh, T.M., Hiroshi, M., Naogutsu, N., Yuki, W., Fumio, Y., Masao, T. (2007) Properties of crosslinked polylactides (PLLA & PDLA) by radiation and its biodegradability. European Polymer Journal, 43, 1779–1785.

[6] Zenkiewicz, M., Rytlewski, P., and Malinowski, R. (2010) Compositional, physical and chemical modification of polylactide. Journal of Achievements in Materials and Manufacturing Engineering, 43, 192–199.

[7] Changgang, X., Xuegang, L., Xiurong, Z., and Lili, L. (2009) Research on Crosslinking of Polylactide using Low Concentration of Dicumyl Peroxide. Materials Science Forum, 620-622, 189-192.

[8] Huang, Y., Zhang, C., Pan, Y., Wang, W., Jiang, L., and Dan, Y. (2013) Study on the effect of Dicumyl Peroxide on Structure and Properties of Poly(Lactic Acid)/Narural Rubber Blend. Journal of Polymers and the Environment, 21, 375-387.

[9] Yang, S.L., Wu, Z.H., Yang, W., and Yang, M.B. (2008) Thermal and mechanical properties of chemical crosslinked polylactide (PLA). Polymer Testing, 27, 957–963.

[10] Henton, D.E., Patrick, G., Jim, L., and Jed, R. Natural Fibers, Biopolymers, and Biocomposites. Polylactic Acid Technology. 4 Nov 2013. <http://www.jimluntllc.com/pdfs/polylactic_acid_technology.pdf>

[11] Tsuji, H. and Ikada, Y. (1999) Stereocomplex formation between enantiomeric poly(lactic acid)s. XI. Mechanical properties and morphology of solution-cast films. Polymer, 40, 6699–6708.

[12] Anderson, K.S. and Hillmyer, M.A. (2006) Melt preparation and nucleation efficiency of polylactide stereocomplex crystallites. Polymer, 47, 2030-2035.

[13] Yokohara, T. and Yamaguchi, M. (2008) Structure and properties for biomass-based polyester blends of PLA and PBS. European Polymer Journal, 44, 677–685.

[14] Ren, J., Hongye, F., Tianbin, R., and Weizhong, Y. (2009) Preparation, characterization and properties of binary and ternary blends with thermoplastic starch, poly(lactic acid) and poly(butylene adipate-co-terephthalate). Carbohydrate Polymers, 77, 576–582.

[15] Chang, L. and Woo, E.M. (2011) Effects of molten poly(3-hydroxybutyrate) on crystalline morphology in stereocomplex of poly(L-lactic acid) with poly(D-lactic acid). Polymer, 52, 68–76.

[16] Bhattacharya, A., Rawlins, J.W., Ray, P. (2009) Polymer Grafting and Crosslinking. Published by John Wiley & Sons, Ins, Inc., Hoboken, New Jersey.

[17] Żenkiewicz, M., Rytlewski, P., and Malinowski, R. (2010) Compositional, physical and chemical modification of polylactide. Journal of Achievements in Materials and Manufacturing Engineering, 43(1), 192-199.

[18] Galagan, Y., Hsu, S.-H., and Su, W.-F. (2010) Monitoring time and temperature by methylene bule containing polyacrylate film. Sensors and Actuators B: Chemical, 144, 49-55.

[19] Ogliari, F.A., Caroline, E., Cesar, H.Z., Carmen, B.B.F., Susana, M.W.S., Fla´ vio, F.D., Cesar, L.P., Evandro, Piva. (2008) Influence of chain extender length of aromatic dimethacrylates on polymer network development. Dental Materials, 24, 165–171.

[20] Ramis, X. and Salla, J.M. (1997) Time-Temperature Transformation (TTT) Cure Diagram of an Unsaturated Polyester Resin. Journal of Polymer Science: Part B: Polymer physics, 35, 371-388.

[21] Zhang, X., Yi, X., and Xu, Y. (2008) Phase separation time/temperature dependence of thermoplastics-modified thermosetting systems. Chemical Engineering of China, 2(3), 276-285.

[22] Winter, H.H. and Chambon, F. (1986) Analysis of Linear Viscoelasticity of a Crosslinking Polylmer at the Gel Point. Journal of Rheology, 30(2), 367-382.

[23] Grillet, A.M., Wyatt, N.B., Gloe, L. M. (2012). Polymer gel rheology and adhesion. Rheology edited by Dr. Juan De Vicente, March 2012 <http://www.intechopen.com>.

[24] Quynh, T.M., Hiroshi, M., Naogutsu, N., Yuki, W., Fumio, Y., Masao, T. (2007) Properties of crosslinked polylactides (PLLA & PDLA) by radiation and its biodegradability. European Polymer Journal, 43, 1779–1785.

[25] Shin, B.Y., Han, D.H., and Narayan, R. (2010) Rheological and Thermal Properties of the PLA Modified by Electron Irradiation in the Presence of Functional Monmer. Journal of Polymers and the Environment, 18, 558-566.

[26] Lee, K.Y., Blaker, J.J. and Bismarch, A. (2009) Surface functionalisation of bacterial cellulose as the route to produce green polylactide nanocomposites with improved properties. Composites Science and Technology, 69, 2724-2733.

[27] Wang, Y., Yang, L., Niu, Y., Wang, Z., Zhang, J., Yu, F., and Zhang, H. (2011) Rheological and Topological Characterization of Electron Beam Irradiation Prepared Long-Chain Branched Polylactic Acid. Journal of Applied Polymer Science, 122, 1857-1865.

[28] Ghosh, K., Shu, X.Z., Mou, R., Lombardi, J., Prestwich, G.D., Rafailovich, M.H., and Clark, R.A.F. (2005) Rheological Characterization of in Situ Cross-Linkable Hyaluronan Hydrogels. Biomacromolecules, 6, 2857-2865.

[29] Huang, Y., Zhang, C., Pan, Y., Wang, W., Jiang, L., and Dan, Y. (2013) Study on the Effect of Dicumyl Peroxide on Structure and Properties of Poly(Lactic Acid)/Natural Rubber Blend. Journal of Polymer Environment, 21, 375-387.

[30] Bhardwaj, R. and Mohanty, A.K. (2007) Modification of Brittle Polylactide by Novel Hyperbranched Polymer-Based Nanostructures. Biomacromolecules, 8, 2476-2484.

[31] Di, Y., Iannace, S., Maio, R.D., and Nicolais, L. (2005) Reactively Modified Poly(lactic acid): Properties and Foam Processing. Macromolecular Materials and Engineering, 290, 1083-1090.

[32] Kim, E.S., Kim, B.C., and Kim, S.H. (2004) Structural Effect of Linear and Star-Shaped Poly(L-lactic acid) on Physical Properties. Journal of Polymer Science: Part B: Polymer physics, 42, 939-946.

[33] Frone, A.N., Berlioz, S., Chailan, J.-F., and Panaitescu, D.M. (2013) Morphology and thermal properties of PLA-cellulose nanofibers composites. Carbohydrate Polymers, 91, 377-384.

[34] Semba, T., Kitagawa, K., Ishiaku, U.S., and Hamada, H. (2006) The Effect of Crosslinking on the Mechanical Properties of Polylactic Acid/Polycaprolactone Blends. Journal of Applied Polymer Science, 101, 1816-1825.